

**N A S A T E C H N I C A L
R E P O R T**



NASA TR R-361

NASA TR R-361

**DESIGN AND GLOBAL ANALYSIS
OF SPACECRAFT ATTITUDE
CONTROL SYSTEMS**

by George Meyer

Ames Research Center

Moffett Field, Calif. 94035

1. Report No. NASA TR R-361	2. Government Accession No.	3. Recipient's Catalog No.	
4. Title and Subtitle DESIGN AND GLOBAL ANALYSIS OF SPACECRAFT ATTITUDE CONTROL SYSTEMS		5. Report Date March 1971	
		6. Performing Organization Code	
7. Author(s) George Meyer		8. Performing Organization Report No. A-3526	
9. Performing Organization Name and Address NASA Ames Research Center Moffett Field, Calif., 94035		10. Work Unit No. 125-19-03-09-00-21	
		11. Contract or Grant No.	
12. Sponsoring Agency Name and Address National Aeronautics and Space Administration Washington, D. C., 20546		13. Type of Report and Period Covered Technical Report	
		14. Sponsoring Agency Code	
15. Supplementary Notes			
16. Abstract <p>A general procedure for the design and analysis of three-axis, large-angle attitude control systems has been developed. Properties of three-dimensional rotations are used to formulate a model of such systems. The model is general in that it is based on those properties which are common to all attitude control systems, rather than on special properties of particular components. Numerical values are assigned to attitude error by means of error functions. These functions are used to construct asymptotically stable control laws. The overall (global) behavior of the system is characterized by the envelope of all time histories of attitude error generated by every possible combination of initial condition, target attitude motion, and disturbance. A method for computing upper bounds on the response envelope is presented. Applications of this method indicate that it provides a useful alternative to Liapunov analysis for the determination of system stability, responsiveness, and sensitivity to disturbances, parameter variations, and target attitude motion.</p>			
17. Key Words (Suggested by Author(s)) Nonlinear Multivariable Stability Sensitivity Computation		18. Distribution Statement Unclassified -- Unlimited	
19. Security Classif. (of this report) Unclassified	20. Security Classif. (of this page) Unclassified	21. No. of Pages 53	22. Price* \$3.00

TABLE OF CONTENTS

	<u>Page</u>
SYMBOLS	v
SUMMARY	1
INTRODUCTION	1
SOME PROPERTIES OF THREE-DIMENSIONAL ROTATIONS	3
Representation of Attitude - Attitude Error Equation	3
Angular Velocity - The Kinematic Equation	5
Parameterization of Attitude Error Matrix	6
Angular Acceleration - The Dynamic Equation	9
Mathematical Model of Attitude Control Systems	11
DESIGN OF CONTROL LAWS	14
GLOBAL ANALYSIS OF SYSTEM PERFORMANCE	22
Response Envelope	22
State Space Interpretation of the Response Envelope	23
COMPUTATION OF RESPONSE ENVELOPES	25
Approximate Computation of Response Envelopes	26
Exact Computation of the Response Envelope	29
Comparison Models for Attitude Control Systems	31
Applications	35
CONCLUDING REMARKS	40
APPENDIX A - METRIC PROPERTIES OF THE ϕ FUNCTION	42
APPENDIX B - KINEMATIC EQUATION IN TERMS OF THE (ϕ, c) PARAMETERS	44
REFERENCES	46

SYMBOLS

\hat{a}	right-hand orthonormal triplet fixed in the controlled body
A_{as}	direction cosine matrix locating \hat{a} with respect to \hat{s}
A_{ds}	direction cosine matrix locating \hat{d} with respect to \hat{s}
c	axis of attitude error; unit eigenvector of R
\hat{d}	right-hand triplet representing target attitude
E^n	the space of real n -tuples
f	the right-hand side of the dynamic equation
h_a	body coordinates of total angular momentum
h_s	inertial coordinates of total angular momentum
h_a^c	angular momentum stored in the device
I	3×3 identity matrix
J_a	body coordinates of body moment of inertia matrix
m	magnitude of attitude error
$m(t, x_0, u)$	time history of attitude error
$m^*(t, x_0)$	time history of attitude error for motion on the boundary of moving cloud
\underline{m}^{**}	response envelope
\underline{m}^+	upper estimate on the response envelope
n_1	kinematic perturbation function
n_2	dynamic perturbation function
p	normal to the boundary of the cloud
R	attitude error matrix
(R, ω_a)	system state, x
\hat{s}	right-hand, orthonormal triplet fixed in inertial space
$S(\cdot)$	skew-symmetric matrix function defined by equation (4)

t	time variable
T_a	body coordinates of external torque
T_a^m	torque generated by the three reaction wheel motors
u	forcing function
u_1	kinematic forcing function
u_2	dynamic forcing function
U	set of admissible values of forcing function
\underline{U}	set of admissible time histories of forcing function
V	function defining the boundary of the cloud
V_t	partial derivative with respect to t
V_x	partial derivative with respect to x
V^+	solution to the Liapunov inequality
x	state variable
X	state space
\underline{X}	set of all possible motions of the system
y_1	kinematic perturbation
y_2	dynamic perturbation
z	nominal control law
β_i	inner gimbal angle of i th star tracker
γ_i	outer gimbal angle of i th star tracker
ϵ	Euler vector defined by equation (19b)
η	Euler parameter defined by equation (19a)
θ	region of system operation
θ_0	set of admissible initial conditions
μ	mode variable
ϕ	attitude error angle
v_i	

$\underline{\phi}^{**}$	response envelope with respect to the error angle
ψ	angle between error axis and angular velocity vector
ω	body coordinates of angular velocity error
ω_a	body coordinates of body angular velocity w.r.t. inertial space
ω_d	target coordinates of target angular velocity w.r.t. inertial space
$()'$	time derivative of $()$
$()^t$	transpose of $()$
$()_x$	partial derivative of $()$ with respect to x
$(_)$	time history
$(\bar{_})$	vector
$\text{sat}(\phi, \phi_s)$	saturation function = ϕ/ϕ_s for $0 \leq \phi \leq \phi_s$ and 1 for $\phi \geq \phi_s$
$\underset{x \in X}{\text{argmax}} f(x)$	that value of x in X which maximizes $f(x)$

DESIGN AND GLOBAL ANALYSIS OF SPACECRAFT

ATTITUDE CONTROL SYSTEMS

George Meyer

Ames Research Center

SUMMARY

A general procedure for the design and analysis of three-axis, large-angle attitude control systems has been developed. Properties of three-dimensional rotations are used to formulate a model of such systems. The model is general in that it is based on those properties which are common to all attitude control systems, rather than on special properties of particular components. Numerical values are assigned to attitude error by means of error functions. These functions are used to construct asymptotically stable control laws. The overall (global) behavior of the system is characterized by the envelope of all time histories of attitude error generated by every possible combination of initial condition, target attitude motion, and disturbance. A method for computing upper bounds on the response envelope is presented. Applications of this method indicate that it provides a useful alternative to Liapunov analysis for the determination of system stability, responsiveness, and sensitivity to disturbances, parameter variations, and target attitude motion.

INTRODUCTION

The complete design of an attitude control system, generally speaking, has four phases; namely, (1) specification of the task to be performed by the system and the selection of major system components; (2) design of the controller linking sensors to torquers; (3) verification of the design; and (4) construction of the system. The present report deals primarily with phases (2) and (3).

One approach to the design of a controller is provided by the theory of optimal control. The methods of this theory are elegant and explicit. Unfortunately, they are difficult to apply when the system is both nonlinear and multidimensional which is the case for large-angle, three-axis attitude control systems being considered here. Not only is the computation of control laws for such systems very time consuming, but the control laws, once computed, are difficult to implement. These difficulties are responsible for the limited enthusiasm shown in the field for the routine application of optimal control theory to the design of control laws for complex systems. Nevertheless, this theory is very useful for the analysis of system performance.

Another approach, which is most frequently taken in practice and, also, the one taken here, is to pick a structure of the control law which on

physical grounds seems most likely to be adequate, and then test the resulting system by means of a computer simulation. The success of this approach depends on two factors: (1) the familiarity of the designer with the general properties of the system, and (2) the validity of the inference that is made from the results of the simulation. The first is obvious. However, the second needs some elaboration, particularly since often it is either overlooked entirely or dismissed as insignificant.

In a simulation one is concerned with accuracy and completeness. A simulation is accurate if the error between the simulated response and the response of the actual system to a given control situation (i.e., initial condition and forcing function) is small. A simulation is complete if the behavior of the system for any possible control situation can be inferred from the collection of cases simulated. If all possibilities are accurately simulated then the simulation is, of course, complete. However, in most cases occurring in practice the number of possible control situations is much larger than is practical to simulate. In such cases, it is necessary to justify the inference that is made in going from the limited collection of tests to the overall (global) behavior of the system. Without this, one cannot be certain that all possible control situations resulting in system failure have been included in the test sample. Thus, the ad hoc design procedure is realistic only if it is followed by a global analysis in which the behavior of the system, or at least an upper bound on the worst case, for all possible control situations is determined analytically. This means that in the selection of candidate control laws the ease with which the subsequent global analysis can be performed must be kept in mind. A control law that is easy to implement and that seems, on physical grounds, to be adequate may, in certain cases, be rejected if it leads to system complexity beyond the reach of the available techniques of global analysis.

Attitude control systems vary considerably in internal structure. Thus, for example, torque may be generated by means of reaction wheels, control moment gyros, or reaction jets. Similarly, attitude may be measured by means of star trackers, sun and magnetic field sensors, or inertial gyros. Angular velocity may be measured directly, as with rate gyros, or it may be computed from attitude data. This variety has resulted in a corresponding variety of control laws, each using special properties of particular components (see, e.g., refs. 1 and 2). In most cases these designs are based on sound physical insight, but they result in systems that are difficult to analyze, and the analysis is not carried out. It is, therefore, desirable to approach the design problem from a general point of view by taking advantage of the basic similarity of all attitude control systems; namely, that (1) their primary control objective is to maintain the spacecraft as close to the desired attitude as is necessary for successful operation, and (2) their basic nonlinearity is that of three-dimensional rotations. This approach was taken in references 3 to 8, and the present report may be considered to be a generalization of that work.

A general model of attitude control systems is formulated from the properties of three-dimensional rotations. Several representations of the distance between the spacecraft and target attitudes are given in terms of

attitude error functions. These functions are used, first, to generate control laws for which the system is asymptotically stable, and then they are used to characterize the overall performance of the system by means of its response envelope. This envelope is defined at each instant in the control interval as the maximum of the attitude error generated by every combination of admissible initial condition, target attitude motion, and disturbance. Worst case performance of the system may be estimated by means of upper bounds on the response envelope. Methods for computing such upper bounds are presented. Finally, the design and analysis are illustrated with examples.

SOME PROPERTIES OF THREE-DIMENSIONAL ROTATIONS

The equations of motion of a spacecraft attitude control system are determined to a large extent by the properties of three-dimensional rotations. Some of these properties are summarized in the present section.

Representation of Attitude - Attitude Error Equation

The attitude of a rigid body may be defined relative to a given reference by means of a pair of right-hand orthonormal triplets of vectors with a common origin 0. Let the triplet $\hat{s} = (\bar{e}_{s1}, \bar{e}_{s2}, \bar{e}_{s3})$ be fixed in the given reference space, and let the triplet $\hat{a} = (\bar{e}_{a1}, \bar{e}_{a2}, \bar{e}_{a3})$ be fixed in the body. In the usual case, the given reference will be inertial space, and the common origin of the triplets will coincide with the body center of mass. Let the transformation which maps \hat{s} into \hat{a} be denoted by \bar{A}_{as} , so that

$$\bar{e}_{ai} = \bar{A}_{as} \bar{e}_{sj}, \quad i = 1, 2, 3 \quad (1)$$

and let \bar{A}_{as} be represented in the s -basis by the 3×3 matrix A_{as} . This matrix will henceforth be interpreted as spacecraft attitude with respect to inertial space. The elements a_{ij} of A_{as} are the direction cosines between \hat{a} and \hat{s} , that is, $a_{ij} = \bar{e}_{ai} \cdot \bar{e}_{sj}$, and the i th row of A_{as} gives the coordinates of \bar{e}_{ai} with respect to \hat{s} . Since both \hat{s} and \hat{a} are right hand and orthonormal, A_{as} is a rotation matrix; that is, $\det(A_{as}) = 1$ and

$$A_{as} A_{as}^t = I \quad (2)$$

where $()^t$ denotes the transpose of $()$, and I is the identity matrix.

Let \bar{x} be an arbitrary vector, and let its coordinates in the s and a basis be x_s and x_a , respectively; then

$$x_a = A_{as} x_s \quad (3)$$

Let \bar{y} be another vector. Then the dot product $\bar{x} \cdot \bar{y} = x_s^t y_s = x_a^t y_a$. Let \bar{z} be the cross product of \bar{x} and \bar{y} ; that is, $\bar{z} = \bar{x} \times \bar{y}$. Then the s coordinates of \bar{z} are given by $z_s = -S(x_s)y_s$, where the skew-symmetric matrix S is defined for any u in E^3 by

$$S(u) = \begin{pmatrix} 0 & u_3 & -u_2 \\ -u_3 & 0 & u_1 \\ u_2 & -u_1 & 0 \end{pmatrix} \quad (4)$$

Similarly, $z_a = -S(x_a)y_a$. Hence, $A_{as}^t S(x_a)A_{as} = S(x_s)$, and, in general, for any x in E^3 and any rotation matrix A ,

$$A^t S(Ax)A = S(x) \quad (5)$$

In addition, the matrix S has the following useful properties. For any u in E^3 ,

$$S^2(u) = -u^t u I + uu^t \quad (6)$$

and for any u and v in E^3 ,

$$S(u)v = -S(v)u \quad (7)$$

and

$$S(u + v) = S(u) + S(v) \quad (8)$$

These relations play an important role in what follows. As an immediate application, consider the problem of measuring A_{as} . Suppose that two inertially fixed directions are given by two unit vectors \bar{x}^1 and \bar{x}^2 . If the inertial coordinates x_s^1, x_s^2 of these vectors are known, and if their body coordinates x_a^1, x_a^2 can be measured, then the attitude matrix A_{as} can be computed as follows. Form the matrix B_s in which the first two columns are x_s^1 and x_s^2 and the third is the cross product $x_s^3 = -S(x_s^1)x_s^2$. Similarly, form the matrix B_a from measurements. Then it follows from equation (3) that $A_{as} = B_a B_s^{-1}$. The inverse of B_s exists whenever the two inertial directions are not colinear. In an actual mechanization, the two inertial directions may be defined by stars, in which case x_s^i are given by star tables, and x_a^i may be computed from star tracker gimbal angles (see example 7 on p. 18).

The target (desired) attitude may be defined by a third right-hand orthonormal triplet of vectors, say $\hat{d} = (\bar{e}_{d1}, \bar{e}_{d2}, \bar{e}_{d3})$ whose origin is common with that of \hat{s} and \hat{a} . The transformation mapping \hat{s} into \hat{d} will be

denoted by \bar{A}_{ds} . Its representation in \hat{s} will be denoted by the matrix A_{ds} and identified as the target attitude. The elements of A_{ds} are the direction cosines $\bar{e}_{di} \cdot \bar{e}_{sj}$.

Consider, now, a way in which attitude error may be defined. When the actual attitude of the spacecraft is the desired attitude, $A_{as} = A_{ds}$. This condition may be expressed either as $A_{as} - A_{ds} = 0$, or as $A_{as}A_{ds}^{-1} = I$, which by orthogonality of A_{ds} is equivalent to $A_{as}A_{ds}^t = I$. Since the ease with which a given set of problems can be solved depends, strongly on the underlying mathematical structure, it is desirable to introduce as much structure at the outset as possible. The set of three-dimensional orthogonal matrices has a well-developed structure. In order to have this structure at hand in what follows, system attitude error will be defined by the orthogonal matrix

$$R = A_{as}A_{ds}^t \quad (9)$$

It may be noted that R represents the rotation from \hat{d} to \hat{a} . The matrices A_{ds} , A_{as} , and R will be referred to as the system input, output, and error, respectively.

Angular Velocity - The Kinematic Equation

Suppose that the spacecraft \hat{a} is rotating with angular velocity $\bar{\omega}$ relative to the inertial space \hat{s} . Let \bar{x} define a point P fixed in the body. Then, $x_a = A_{as}x_s$, $\dot{x}_a = 0$, and $\dot{x}_s = -S(\omega_s)x_s$. Hence, the following chain of equations is true,

$$0 = \dot{x}_a = \dot{A}_{as}x_s + A_{as}\dot{x}_s = [\dot{A}_{as}A_{as}^t - A_{as}S(\omega_s)A_{as}^t]x_a = [\dot{A}_{as}A_{as}^t - S(\omega_a)]x_a$$

Since this chain is true for any fixed point P , it follows that,

$$\dot{A}_{as} = S(\omega_a)A_{as} \quad (10)$$

This is the kinematic equation of spacecraft attitude. The corresponding equation for the target is

$$\dot{A}_{ds} = S(\omega_d)A_{ds} \quad (11)$$

The attitude error is defined by (9). Hence, $\dot{R} = \dot{A}_{as}A_{ds}^t + A_{as}\dot{A}_{ds}^t$, and from equations (10) and (11) it follows that

$$\dot{R} = S(\omega_a)R - RS(\omega_d) \quad (12)$$

This is the kinematic equation of attitude error. Note that equation (12) is a well-behaved differential equation. It is defined for all attitude errors; it is without singularities; and, for given time histories of spacecraft and target angular velocities, it is linear. According to equation (5), $RS(\omega_d) = S(R\omega_d)R$; hence, equation (12) is equivalent to the following equation which is useful for certain purposes.

$$\dot{R} = S(\omega_a - R\omega_d)R \quad (13)$$

The argument of S in (13), $\omega_a - R\omega_d = \omega$, can be interpreted as the coordinates of angular velocity error.

Parameterization of Attitude Error Matrix

The elements of R are not independent; they are connected by the orthogonality condition $RR^t = I$. Thus, R may be parameterized with fewer than nine parameters. The minimum number is three (i.e., Euler angles). However, the minimum number is not always convenient. A particularly useful parameterization is the following.

Suppose that \hat{a} , originally coincident with \hat{d} , is rotated with a constant angular velocity $\bar{\alpha}$ relative to \hat{d} . Then $R(0) = I$, and $\dot{R}(t) = S(\alpha)R(t)$, where $\bar{\alpha}$ is constant. This is a linear differential equation with constant coefficients whose solution is $R(t) = \exp[S(\alpha)t]$. Let $\phi = \|\alpha\|t$ and $c = \alpha/\|\alpha\|$, so that $\|c\| = 1$. Then

$$R = \exp[\phi S(c)] \quad (14)$$

The scalar ϕ will be interpreted as the magnitude of attitude error, and the unit vector c will be interpreted as the direction of attitude error. Expanding the exponential in equation (14), and noting from equation (6) that $S^3(c) = -S(c)$, and so on for higher powers of S , and collecting terms yields the following equivalent expression of equation (14):

$$R = I + \sin \phi S(c) + (1 - \cos \phi)S^2(c) \quad (15)$$

Since $S(c)c = 0$, c is an eigenvector of R ; that is, $Rc = c$. The corresponding eigenvalue is 1. It is the consequence of Euler's theorem on rotations that any attitude can be reached from I by a constant angular velocity. Hence, any R can be parameterized by (ϕ, c) as in equation (14) and its equivalent equation (15).

The parameters (ϕ, c) can be computed from the elements r_{ij} of R expressed by equation (15). Thus, since $\text{trace } S(c) = 0$, and $\text{trace } S^2(c) = -2$, $\text{trace}(R) = 3 - 2(1 - \cos \phi)$; hence,

$$\phi = \arcsin \left\{ \frac{1}{2} [\text{trace}(R) - 1] \right\}_{[0, \pi]} \quad (16)$$

where $[0, \pi]$ is the closed interval from 0 to π . On the other hand, since both I and $S^2(c)$ are symmetric, $\sin \phi S(c) = (1/2)(R - R^t)$. Hence, for $0 < \phi < \pi$,

$$c = \frac{1}{2 \sin \phi} \begin{pmatrix} r_{23} - r_{32} \\ r_{31} - r_{13} \\ r_{12} - r_{21} \end{pmatrix} \quad (17)$$

The cases $\phi = 0, \pi$ are singular. When $\phi = 0$, c is arbitrary. When $\phi = \pi$, equation (15) shows that the components of c are the solutions to the following equations.

$$|c_i| = \left[\frac{1}{2} (r_{ii} + 1) \right]^{1/2}, \quad c_i c_j = \frac{1}{2} r_{ij} \quad (17a)$$

The error angle function ϕ defined by equation (16) has several useful properties, which are listed below.

(i) In the one-dimensional case (i.e., shaft positioning servo), in which c is constant, the usual definition of error is $\phi_e = \phi_d - \phi_a$, where ϕ_d and ϕ_a are input and output angles, respectively. In that case $\phi = |\phi_e|$ if $|\phi_e| \leq \pi$, and $\phi = 2\pi - |\phi_e|$ if $\pi \leq \phi_e \leq 2\pi$.

(ii) When ϕ is small, the attitude error may be represented by the vector ϕc . Its components are, to first order, Euler angles of R , and ϕ is the square root of the sum of the squares of these angles.

(iii) Let θ_i be the angle between the i th vector of \hat{a} and the i th vector of \hat{d} . Then $\theta_i \leq \phi$, because $r_{ii} = \cos \theta_i = \cos \phi + (1 - \cos \phi)c_i^2$ which implies that $\cos \theta_i \geq \cos \phi$.

(iv) Consider all paths from I to R . Each satisfies the differential equation $\dot{R} = S[\omega(t)]R$ for some time history $\underline{\omega}$ and boundary conditions $R(0) = I$, $R(t_f) = R$. It can be shown (see appendix A) that for all $\underline{\omega}$,

$$\phi \leq \int_0^{t_f} \|\omega(t)\| dt$$

so that ϕ may be considered to be the minimum angular distance between \hat{a} and \hat{d} . This also means that for any two orthogonal (three-dimensional) matrices A and B , $\phi(AB^t) \leq \phi(A) + \phi(B)$. In fact, the function $\phi(A, B) = \phi(AB^t)$ is a metric on the space of three-dimensional rotation matrices: (1) $\phi(A, B)$ is positive; (2) $\phi(A, B) = 0$ if and only if $A = B$; (3) $\phi(A, B) = \phi(B, A)$; and (4) $\phi(B, A) + \phi(A, C) \geq \phi(B, C)$.

Consider, next, the kinematic equation in terms of (ϕ, c) . It is shown in appendix B that for any ϕ , c , and ω

$$\dot{\phi} = c^t \omega \quad (18a)$$

$$\dot{c} = \frac{1}{2} S(\omega) c + \frac{1}{2} \cot\left(\frac{1}{2} \phi\right) [\omega - (\omega^t c) c] \quad (18b)$$

Equations (18) are singular at $\phi = 0$ and $\phi = \pi$. To gain some insight into the properties of equations (18) consider the special case in which the angular velocity ω is a constant unit vector. Let the angle between c and ω be denoted by ψ . Then, according to equation (18a), $\dot{\phi} = \cos \psi$, and from equation (18b), $(\cos \psi)' = (1/2) \cot[(1/2)\phi] \sin^2 \psi$. Hence, the motion passing through the point (ϕ_0, ψ_0) remains on the curve

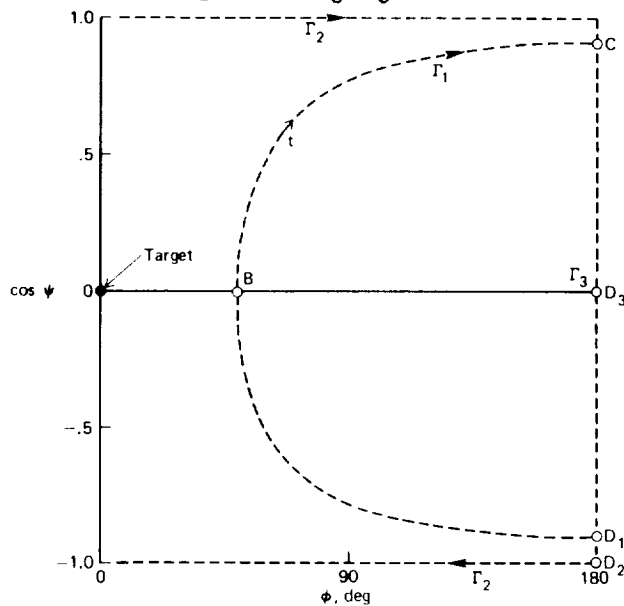


Figure 1.— Motion of system with constant angular velocity.

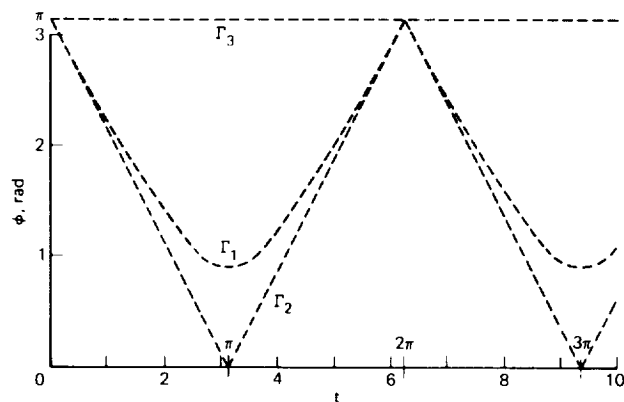


Figure 2.— Time histories of error angle for constant angular velocity.

$$\sin\left(\frac{1}{2} \phi\right) \sin \psi = \sin\left(\frac{1}{2} \phi_0\right) \sin \psi_0$$

Curves corresponding to three different initial conditions are sketched in figure 1. Curve Γ_1 is at the point D_1 at time $t = 0$. As the body rotates about ω , it swings by the target. The closest approach is at point B where $\phi = 50^\circ$ and c is perpendicular to ω . Thereafter, ϕ increases until $\phi = 180^\circ$ (point C) where c switches sign (point D_1). The body then begins to approach the target ($\phi = 0$) repeating the cycle. If c is colinear with ω at $t = 0$ (point D_2), it remains so for all time, switching sign of c at $\phi = 0^\circ$ and $\phi = 180^\circ$ (curve Γ_2). Finally, if at $t = 0$, $\phi = 180^\circ$ and c is perpendicular to ω (point D_3), then the body never approaches the target but remains always at the maximum distance away (point Γ_3). Figure 2 shows the time histories of the error angle ϕ corresponding to these three cases.

The singularity at $\phi = 0$ can be removed by multiplying c by a suitable function of ϕ . For example, Euler parameters (η, ϵ) are defined as follows.

$$\eta = 2 \cos \left(\frac{1}{2} \phi \right) \quad (19a)$$

$$\epsilon = 2 \sin \left(\frac{1}{2} \phi \right) c \quad (19b)$$

These parameters are related by the equation $\eta^2 + \epsilon^2 = 4$. The corresponding kinematic equation may be obtained from equations (18). It is the following set.

$$\dot{\eta} = -\frac{1}{2} \epsilon \omega \quad (20a)$$

$$\dot{\epsilon} = \frac{1}{2} S(\omega) \epsilon + \frac{1}{2} \eta \omega \quad (20b)$$

Euler parameters have the advantage that the corresponding kinematic equations (20) is continuous at $\phi = 0$, and it does not involve trigonometric functions. However, the singularity at $\phi = \pi$ is still present.

There are other parameterizations of three-dimensional rotations, but since they will not be used in this report, they will not be discussed.

Angular Acceleration - The Dynamic Equation

The motion of the spacecraft about the fixed point 0 may be influenced in two ways: By means of external torques (i.e., reaction jets); and by means of internal torques generated by an angular momentum exchange and storage device (i.e., reaction wheels, control moment gyros). In general, both influences may be present. Let the angular momentum of the main body (about the fixed point 0) and that stored in the exchange device be denoted by the vectors \bar{h}^v and \bar{h}^c , respectively, and let \bar{T} be the total external torque acting on the system. The total angular momentum $\bar{h} = \bar{h}^v + \bar{h}^c$, and the time derivative of its inertial coordinates is, according to Newton's law,

$$\dot{\bar{h}}_s = \bar{T}_s = A_{as}^t \bar{T}_a \quad (21)$$

Let the a-coordinates of the moment of inertia of the main body be denoted by the matrix J_a . Then in \hat{a} ,

$$\bar{h}_a = J_a \omega_a + \bar{h}_a^c$$

But $\bar{h}_a = A_{as} \bar{h}_s$, and according to equation (6) $\dot{A}_{as} = S(\omega_a) A_{as}$. Hence,

$$\begin{aligned} \dot{\bar{h}}_a &= S(\omega_a) A_{as} \bar{h}_s + \bar{T}_a \\ &= \dot{J}_a \omega_a + J_a \dot{\omega}_a + (\bar{h}_a^c)' \end{aligned}$$

Therefore,

$$\dot{\omega}_a = J_a^{-1}(-h_a^C)' + J_a^{-1}T_a + J_a^{-1}S(\omega_a)A_{as}h_s - J_a^{-1}\dot{J}_a\omega_a \quad (22)$$

The following interpretations will be given to the terms on the right hand side of (22). The first term represents the effect of angular momentum exchange rate. The second term represents the effect of external torque. The third represents gyroscopic coupling. The fourth is due to time variation of body moment of inertia. Equations (21) and (22) together constitute the system dynamic equation. Its form is useful for control applications because the variables $(-h_a^C)'$, T_a , and \dot{J}_a appear explicitly, and they are the ones usually available for control. The following special cases appear frequently in practice.

Case 1 - external torque- Suppose that the angular momentum exchange and storage device is inactive so that $h_a^C = 0$, for all $t \geq 0$, and that the moment of inertia J_a is constant. Then $h_a = A_{as}h_s = J_a\omega_a$, and the dynamic equation is the Euler's equation of motion,

$$\dot{\omega}_a = J_a^{-1}T_a + J_a^{-1}S(\omega_a)J_a\omega_a \quad (23)$$

The control variable is the external torque T_a . It is typically generated by means of reaction jets, external magnetic field, gravity gradient, etc.

Case 2 - reaction wheels- Suppose that the system is being controlled by means of an angular momentum exchange and storage device consisting of three reaction wheel-motor pairs placed along the body axes \hat{a} . Let J_a^V be the moment of inertia of the main body with locked wheels; let J_a^W be the diagonal matrix whose elements are the moments of inertia of the wheels about their spin axes, and let T_a^m be the column matrix whose elements are the wheel motor torques. Then defining $J_a = J_a^V - J_a^W$, and assuming no external torque and constant J_a , it follows that

$$\dot{\omega}_a = J_a^{-1}T_a^m + J_a^{-1}S(\omega_a)A_{as}h_s \quad (24)$$

where h_s is a constant. In this case the control variable is the motor torque T_a^m .

Case 3 - control moment gyros- Suppose that the system is being controlled by means of a set of control moment gyros. Let the active gimbal angles of all the gyros in the package be arranged in a column matrix q of an appropriate dimension, and let the a -coordinates of the total angular momentum of all gyros be denoted by h_a^C . Assuming that the total angular momentum of each gyro may be adequately represented by its spin momentum, we may express h_a^C as a function of q , say, $h_a^C = h(q)$. Then $(h_a^C)' = h_q(q)\dot{q}$, and

for $T_a = 0$ and constant J_a , the dynamic equation is given by

$$\dot{\omega}_a = J_a^{-1}[-h_q(q)]\dot{q} + J_a^{-1}S(\omega_a)A_{as}h_s$$

where h_s is a constant. Suppose that the gimbal angles are driven through a processor so that

$$\dot{q} = -F(q)J_a e$$

where e is the input to the processor. Then

$$\dot{\omega}_a = J_a^{-1}h_q(q)F(q)J_a e + J_a^{-1}S(\omega_a)A_{as}h_s \quad (25)$$

In this case e is the control variable. If h is a one to one mapping from the region of interest Q onto $h(Q)$ and the processor is such that $F(q) = h_q^{-1}(q)$, then (25) acquires a particularly simple form.

Equations (11), (13), (21), and (22) describe the system. For given initial condition and time histories of the control variables, the motion of the system is the corresponding solution of these equations. The detailed mathematical model is considered in the following section.

Mathematical Model of Attitude Control Systems

The discussion in the preceding section motivates the mathematical model of attitude control systems shown in table 1. The model might appear at first sight unnecessarily detailed; however, it is basically quite simple and useful for the purposes of the following discussion. The detail given is required by the analytical techniques to be employed.

TABLE 1.- MATHEMATICAL MODEL OF ATTITUDE CONTROL SYSTEMS

State space	$X = E^{12}, \quad x = (R, \omega_a)$
Region of operation	$\theta = \{x: RR^t = I \text{ and } \det(R) = 1\}$
Admissible initial conditions	$\theta_0 \subset \theta$
State equation	$\dot{x} = g[t, x, u(t), \mu]$
Kinematic equation	$\dot{R} = S(\omega_a + y_1)R$
Dynamic equation	$\dot{\omega}_a = f(t, x, \mu, y_2)$
Nominal control law	$f(t, x, \mu, 0)$
Mode variable	μ
Perturbations	
Target velocity	$y_1 = n_1(t, x, \mu)u_1(t)$
Disturbance	$y_2 = n_2(t, x, \mu)u_2(t)$
Admissible forcing functions	$(\underline{u}_1, \underline{u}_2) \in \underline{U}$

The underlying state space X is 12-dimensional with the state x denoted mnemonically by (R, ω_a) . The first nine components of x are the elements of the error matrix R , and the remaining three coordinates are the body (\hat{a}) coordinates of body angular velocity ω_a . The region of operation θ of the system is the 6-dimensional manifold defined by the condition that R be a rotation matrix. All possible motions of the system are inherently restricted to this θ . The reason for imbedding the system in E^{12} is to have a nonsingular kinematic equation. The set of admissible initial conditions θ_0 , which contains all possible states of the system at the time of the initiation of control, is a closed subset of θ . The state equation consists of the kinematic equation and the dynamic equation. There are two types of perturbation: y_1 represents target angular velocity; y_2 represents disturbances entering through the dynamic equation. The system will be said to be under the action of the nominal control law when $y_2 = 0$. In general, the system may operate in any one of several modes. A system with several star trackers is typical. In certain mechanizations the form of control law depends on which star trackers are active. Hence, in such systems there are as many modes as star tracker combinations. The mode is represented in table 1 by the mode variable μ . It will be assumed that the number of modes is finite, that with each mode there is associated an open subset θ_μ of θ , and that these subsets cover θ . The perturbations y_1 and y_2 are given in terms of intensities n_1 and n_2 and forcing functions u_1 and u_2 . The combined forcing function $\underline{u} = (\underline{u}_1, \underline{u}_2)$ is restricted to the set of piecewise continuous vector functions of time with values in U . This set is denoted in table 1 by \underline{U} . Finally, the functions f , n_1 , and n_2 are assumed to be continuous on the closure of θ_μ for each μ .

The following examples illustrate how specific cases may be described by the model of the type shown in table 1.

Example 1- Suppose that initial attitudes of both the spacecraft and target are arbitrary, that initial spacecraft angular velocity is spherically bounded by a given constant ω_{amax} , but otherwise arbitrary, and that target angular velocity is spherically bounded by ω_{dmax} for all $t > 0$, but otherwise arbitrary. Then, the set of admissible initial conditions θ_0 in table 1 may be defined by (see eq. (16))

$$\theta_0 = \{x: 0 \leq \phi \leq \pi, \|\omega_a\| \leq \omega_{amax}\}$$

and the target angular velocity perturbation may be accounted for by

$$n_1 = \omega_{dmax}, \quad \|u_1\| \leq 1$$

The form of the dynamic equation depends on the way torque is generated. Suppose that the spacecraft is being controlled by means of reaction wheels (see eq. (24)), and that the total angular momentum of the system $h_s = 0$. Suppose, also that the feedback linking the sensors to wheel motors is given by

$$T_a^m = z(R, \omega_a, \mu)$$

where z is a specific function. Then the function f in the dynamic equation in table 1 is given by

$$f = J_a^{-1} z(R, \omega_a, \mu) + y_2$$

while the intensity of perturbation in this case is

$$n_2 = 0$$

Example 2- Suppose that the situation is as in example 1, except that the control is by means of control moment gyros (see eq. (25)). Let the input e to the processor be given by

$$e = z(R, \omega_a, \mu)$$

and let the perturbation function be defined as

$$n_2 = \max_Q \|I - J_a^{-1} h_q(q) F(q) J_a\| \|z(R, \omega_a, \mu)\|, \quad \|u_2\| \leq 1 \quad (26)$$

This gives the maximum deviation from the nominal control law $z(R, \omega_a, \mu)$. Then the system can be modeled by setting

$$f = z + y_2$$

The resulting model in table 1 represents the system in the sense that all possible motions of the systems are included in the set of all possible motions of the model.

Example 3- Suppose that the spacecraft is controlled by means of an angular momentum exchange and storage device as in example 1, and that an angular momentum dumping scheme is employed. The corresponding dynamic equation is given by equation (22). Let the dumping torque be spherically bounded by T_{\max} , and let the total angular momentum h_s be spherically bounded by $h_{s\max}$. Then, assuming that $(h_a^C)' = -z(R, \omega_a, \mu)$, the system can be represented in the form of table 1 by setting

$$f = J_a^{-1} z(R, \omega_a, \mu) + y_2$$

$$y_2 = n_2 u_2$$

where n_2 is the 3×6 matrix

$$n_2 = [T_{\max} J_a^{-1}, h_{s\max} J_a^{-1} S(\omega_a)] \quad (27)$$

and where the forcing vector is six-dimensional,

$$u_2 = \begin{pmatrix} u_2^1 \\ \text{---} \\ u_2^2 \end{pmatrix}, \quad \|u_2^i\| \leq 1 \quad \text{for } i = 1, 2$$

DESIGN OF CONTROL LAWS

The direct synthesis of control laws by means of optimal control theory is often impractical because of the attending computational difficulties and because the resulting laws are difficult to implement. An alternative approach is to pick a feedback structure which on physical grounds is likely to result in adequate system performance, and then perform a global analysis to determine whether the performance is, in fact, adequate. The latter approach is taken in the present report. A method for generating a class of candidate control laws is presented in the present section. The system governed by any member of this class is shown to be asymptotically stable. Further global properties of the system may be determined by the techniques developed in the succeeding sections.

Suppose that the target attitude is constant ($\underline{\omega}_d = \underline{0}$) so that the kinematic equation (13) is

$$\dot{R} = S(\omega_a)R \quad (28a)$$

and that the controls are adjusted so that the dynamic equation (22) is

$$\dot{\omega}_a = z(x) \quad (28b)$$

where z is a control law to be selected, and $x = (R, \omega_a)$ is the state. The method for generating candidate control laws to be now discussed is based on the following simple example.

Choose the magnitude of attitude error to be the following function of R

$$m(R) = \frac{1}{2} \phi^2 \quad (29a)$$

where the error angle ϕ is defined by equation (16). The time rate of change of m along any trajectory of the system (28) is, according to equation (18a),

$$\dot{m} = (\phi c)^t \omega_a \quad (29b)$$

Let the control law be given by

$$z(x) = -\phi c - \omega_a \quad (29c)$$

Then the system (28) is asymptotically stable on the set

$$\theta_0 = \left\{ x: m + \frac{1}{2} \omega_a^t \omega_a \leq a \right\}$$

for any a in the half-open interval $[0, (1/2)\pi^2)$. The function $V = m + (1/2)\omega_a^t \omega_a$ is a Lyapunov function for the process: V is a positive definite, and its time derivative along any trajectory, $\dot{V} = \phi c^t \omega_a - \omega_a^t \phi c - \omega_a^t \omega_a$, is negative for $\omega_a \neq 0$, and if $\omega_a = 0$, then $z \neq 0$, unless also ϕ , or equivalently m , is zero.

The control law (29c) has been generated from the error function (29a) in the following sense. The procedure was to pick a function m that characterizes the magnitude of the three-axis attitude error. Its time derivative turned out to be a linear function of ω_a , namely $(\phi c)^t \omega_a$. This function (covector) $(\phi c)^t$ was converted into a vector ϕc and taken as the attitude error feedback portion of the control law. Finally, rate feedback was added for damping.

Such construction can be carried out in general because the kinematic equation (28a) is linear in ω_a . Thus, let $s(R)$ be a differentiable function of R on the region of interest. If \dot{s} is bounded for all s of interest, then because of linearity of (28a), there is a matrix $F(s)$ such that along any trajectory of the system $\dot{s} = F(s)\omega_a$. Choose a differentiable nesting function $m(s)$ that assigns the notion of magnitude to attitude error in terms of s ; that is, if $a \leq b$ then $\{x: m[s(R)] \leq a\} \subset \{x: m[s(R)] \leq b\}$. The time rate of change of m along any trajectory is $\dot{m} = m_s(s)F(s)\omega_a$. If for all $m \leq m_0$, $m_s(s)F(s) = 0$ only at $m = 0$, then the system (28) controlled by

$$z(x) = -F^t(s)m_s^t(s) - G(s, \omega_a)\omega_a \quad (30)$$

where G is a positive definite matrix, is asymptotically stable with respect to m on the set $\theta_0 = \{x: m + (1/2)\omega_a^t \omega_a \leq m_0\}$. A Liapunov function is $V = m + (1/2)\omega_a^t \omega_a$. The time derivative, $\dot{V} = -\omega_a^t G \omega_a$, is by assumption negative for $\omega_a \neq 0$. For $\omega_a = 0$, $z \neq 0$ unless attitude error feedback is also zero,

which by assumption occurs only at $m = 0$. Hence, any initial condition in θ_0 will be driven to $(m = 0, \omega_a = 0)$. This may be, depending on m , a set in θ - see example 5.

Example 4 - eigenvector control- Let $m(R) = \int_0^\phi g(q) dq$, where $qg(q) > 0$ for $q \neq 0$. This error function generates the following control law.

$$z(x) = -g(\phi)c - G(x)\omega_a \quad (31)$$

The attitude error feedback vector is along the eigenvector c of the error matrix R . In particular, let $g(\phi) = 2k \sin[(1/2)\phi]$, where k is a constant. Then the attitude error feedback becomes $-k\varepsilon$, where ε is the Euler vector defined by (19b).

Example 5- The problem is to align a unit vector \bar{b} fixed in the spacecraft with the unit vector \bar{d} fixed in inertial space. Let the spacecraft coordinates of these vectors be denoted by b_a and d_a , and let their inertial coordinates be denoted by b_s and d_s . In this case, b_a and d_s are constant and d_a is measured. A solution to this problem may be obtained by choosing the error function to be, for some positive constant k_1 ,

$$m = k_1(1 - d_a^t b_a) \quad (32)$$

Then, since $d_a = A_{as}d_s$, and using the kinematic equation (10), it follows that

$$\dot{m} = k_1 d_a^t S(\omega_a) b_a = -k_1 d_a^t S(b_a) \omega_a$$

If G in equation (30) is taken to be another positive constant k_2 , the following control law results

$$z(x) = -k_1 S(b_a) d_a - k_2 \omega_a \quad (33)$$

It may be noted that $k_1 S(b_a)$ is a constant matrix. The system will align \bar{b} along \bar{d} for any initial condition in the set defined by $m + (1/2)\omega_a^t \omega_a < k_1$. Note that m is semidefinite since rotation about \bar{d} is irrelevant; hence, $m = 0$ on a set in θ . The chosen magnitude function can be written as $m = 1 - \cos \theta$, where θ is the angle between \bar{b} and \bar{d} . So, m measures the angle between the two vectors. Suppose that m were defined as the magnitude of the difference $\bar{b} - \bar{d}$; that is, let $m_1 = (1/2)(d_a - b_a)^t (d_a - b_a)$. Expanding this product and noting that \bar{b} and \bar{d} are unit vectors, it follows that $m_1 = 1 - d_a^t b_a = m$, and the same cross product control results.

In certain cases linear control is undesirable because it may require excessive torques for large errors. Nonlinear gains may be introduced to account for torque saturation as follows. Let $s = d_a - b_a$, and choose the magnitude function of s to be

$$m = \sum_1^3 \int_0^{s_i} g_i(q) dq$$

with $qg_i(q) > 0$ for $q \neq 0$. Then the time rate of change of m is

$$\dot{m} = \sum_1^3 g_i(s_i) \dot{s}_i$$

But, $\dot{s} = -S(d_a)\omega_a$, which leads to the following control law.

$$z = S(d_a) \begin{pmatrix} g_1(d_{a1} - b_{a1}) \\ g_2(d_{a2} - b_{a2}) \\ g_3(d_{a3} - b_{a3}) \end{pmatrix} - k_2\omega_a$$

In particular, if all g_i are the same saturation function $ksat(q, q_s)$ which is linear for $|q| \leq q_s$, and saturates at the value k for $|q| \geq q_s$, then the attitude error portion of the feedback is bounded on each axis by k .

Example 6- It is assumed that complete attitude control is desired. Two unit vectors \bar{b}^1, \bar{b}^2 fixed in the spacecraft are to be aligned with two unit vectors \bar{d}^1, \bar{d}^2 fixed in inertial space. The spacecraft is on target (i.e., $R = I$) when $\bar{b}^i = \bar{d}^i$, $i = 1, 2$. It is assumed that the body coordinates of \bar{d}^i are measured by on-board sensors (i.e., a sun sensor and a magnetic field sensor). Let $s^i = d_a^i - b_a^i$, $i = 1, 2$, and choose the magnitude function of attitude error to be

$$m = \sum_1^3 \left[\int_0^{s_i^1} g_i(q) dq + \int_0^{s_i^2} h_i(q) dq \right]$$

with $qg_i(q) > 0$ and $qh_i(q) > 0$ for $q \neq 0$. This error function generates the following control law

$$z = S(d_a^1) \begin{pmatrix} g_1(d_{a1}^1 - b_{a1}^1) \\ g_2(d_{a2}^1 - b_{a2}^1) \\ g_3(d_{a3}^1 - b_{a3}^1) \end{pmatrix} + S(d_a^2) \begin{pmatrix} h_1(d_{a1}^2 - b_{a1}^2) \\ h_2(d_{a2}^2 - b_{a2}^2) \\ h_3(d_{a3}^2 - b_{a3}^2) \end{pmatrix} - G\omega_a$$

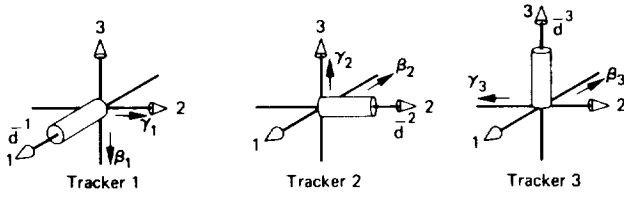


Figure 3.— Arrangement of star trackers. Body axes are numbered; \bar{d}^i are lines of sight; β_i are inner gimbal angles; γ_i are outer gimbal angles.

If the attitude error feedback is zero only at the point $R = I$ of the region $m \leq v$, then the system is asymptotically stable on the region $m + (1/2)\omega_a^t \omega_a < v$.

Example 7— It is assumed that spacecraft attitude is measured with a set of star trackers whose arrangement in the body is shown in figure 3. The body coordinates of lines of sight are,

$$d_a^1 = \begin{pmatrix} c\gamma_1 c\beta_1 \\ -s\beta_1 \\ -s\gamma_1 c\beta_1 \end{pmatrix}, \quad d_a^2 = \begin{pmatrix} -s\gamma_2 c\beta_2 \\ c\gamma_2 c\beta_2 \\ -s\beta_2 \end{pmatrix}, \quad d_a^3 = \begin{pmatrix} -s\gamma_3 c\beta_3 \\ s\beta_3 \\ c\gamma_3 c\beta_3 \end{pmatrix}$$

The corresponding kinematic equations are,

$$\begin{pmatrix} \dot{\beta}_1 \\ \dot{\gamma}_1 \end{pmatrix} = \begin{pmatrix} s\gamma_1 & 0 & c\gamma_1 \\ -c\gamma_1 t\beta_1 & -1 & s\gamma_1 t\beta_1 \end{pmatrix} \omega_a$$

$$\begin{pmatrix} \dot{\beta}_2 \\ \dot{\gamma}_2 \end{pmatrix} = \begin{pmatrix} c\gamma_2 & s\gamma_2 & 0 \\ s\gamma_2 t\beta_2 & -c\gamma_2 t\beta_2 & -1 \end{pmatrix} \omega_a$$

$$\begin{pmatrix} \dot{\beta}_3 \\ \dot{\gamma}_3 \end{pmatrix} = \begin{pmatrix} c\gamma_3 & 0 & s\gamma_3 \\ s\gamma_3 t\beta_3 & 1 & -c\gamma_3 t\beta_3 \end{pmatrix} \omega_a$$

Consider, first, the use of all three trackers. Let s be the inner gimbal angle error, $s_i = \beta_i - \beta_i^0$, $i = 1, 2, 3$. Superscript 0 denotes the target values. Choose

$$m(s) = \sum_1^3 \int_0^{s_i} g_i(q) dq$$

where $qg_i(q) > 0$ for $q \neq 0$. This error function generates the following control law.

$$z = - \begin{pmatrix} s\gamma_1 & c\gamma_2 & c\gamma_3 \\ 0 & s\gamma_2 & 0 \\ c\gamma_1 & 0 & s\gamma_3 \end{pmatrix} \begin{pmatrix} g_1(\beta_1 - \beta_1^0) \\ g_2(\beta_2 - \beta_2^0) \\ g_3(\beta_3 - \beta_3^0) \end{pmatrix} - G\omega_a \quad (34)$$

If in the region $m(s) \leq v$, $\gamma_2 \neq 0$, π and $\gamma_1 + \gamma_2 \neq \pm\pi/2$, then the system is asymptotically stable with respect to $R = I$, in the region $m(s) + (1/2)\omega_a^t \omega_a \leq v$. It may be noted that the resulting control law may be simple to implement: the elements of the gain matrix are provided by resolvers attached to outer gimbals of trackers.

Now, consider only trackers 1 and 3. Let

$$s^t = (\beta_1 - \beta_1^0, \gamma_1 - \gamma_1^0, \beta_3 - \beta_3^0, \gamma_3 - \gamma_3^0)$$

and again choose the error function to be

$$m(s) = \sum_1^4 \int_0^{s_i} g_i(q) dq$$

It generates the control law,

$$z = - \begin{pmatrix} s\gamma_1 & -c\gamma_1 t\beta_1 & c\gamma_3 & s\gamma_3 t\beta_3 \\ 0 & -1 & 0 & 1 \\ c\gamma_1 & s\gamma_1 t\beta_1 & s\gamma_3 & -c\gamma_3 t\beta_3 \end{pmatrix} \begin{pmatrix} g_1(\beta_1 - \beta_1^0) \\ g_2(\gamma_1 - \gamma_1^0) \\ g_3(\beta_3 - \beta_3^0) \\ g_4(\gamma_3 - \gamma_3^0) \end{pmatrix} - G\omega_a \quad (35)$$

If in the region $m(s) \leq v$, $\beta_1 \neq \pm\pi/2$, $\beta_3 \neq \pm\pi/2$, and $\gamma_1 + \gamma_3 \neq \pm\pi/2$, then the resulting system is asymptotically stable with respect to m on the set of initial conditions $m(s) + (1/2)\omega_a^t \omega_a \leq v$. If, in addition the two lines of sight are independent, then $m \rightarrow 0$ implies $R \rightarrow I$. This control law is harder to implement than the preceding one because of the presence of the tangents of inner gimbal angles in the gain matrix. If the terms involving tangents are set to zero, the attitude error feedback becomes that used in an actual Orbiting Astronomical Observatory (OAO). The effect on system performance of this change may be investigated by the techniques presented in the following sections (see example 10).

The final example of this section illustrates the design using actual hardware.

Example 8- It is assumed that the spacecraft is similar to an OAO. The control is by means of reaction wheels. The angular momentum storage capacity of each wheel is $h_{\max} = 4.68$ (N-m-sec); the torque capacity of each wheel motor is $T_{\max} = 0.231$ (N-m). The moment of inertia of the main body is diagonal: $J_a = \text{diag}(999; 1110; 1410)$ (kg-m²). An angular momentum dumping scheme is assumed which maintains the total angular momentum spherically bounded by $h_{s\max} = 1.00$ (N-m-sec). Hence, the wheels will not saturate if body angular velocity ω_a is kept spherically bounded by

$$\begin{aligned}\omega_{a\max} &= (h_{\max} - h_{s\max})/j_{\max} \\ &= 2.61 \text{ (mrad/sec)}\end{aligned}$$

where j_{\max} is the maximum principal moment of inertia of the main body. Finally, it is assumed that on-board sensors measure the attitude error R and body angular velocity ω_a . The problem is to design a control law for stable attitude regulation.

Choose the magnitude function of R to be

$$m(R) = \int_0^\phi k_1 \text{sat}(q, q_s) dq$$

It generates the control law

$$z(x) = -k_1 \text{sat}(\phi, \phi_s) c - k_2 \omega_a \quad (36)$$

Let $k_1 = k_2 \omega_{a\max}$. Then $\|\omega_a\|' \leq 0$ for $\|\omega_a\| \geq \omega_{a\max}$. Hence, the control will not drive the wheels into saturation. Let $k_1 + k_2 \omega_{a\max} = T_{\max}/j_{\max}$. Then if the control law is implemented by setting the wheel motor torques $T_a^m(x) = J_a z(x)$, the motors will not be driven into saturation. Finally, choose the saturation point ϕ_s so as to have damping $\zeta = 0.5$ near $\phi = 0$. This specifies the control law completely. It may be noted that since

$$\text{sat}(\phi, \phi_s) c = \frac{\text{sat}(\phi, \phi_s)}{2 \sin \phi} \begin{pmatrix} r_{23} - r_{32} \\ r_{31} - r_{13} \\ r_{12} - r_{21} \end{pmatrix}$$

the control law (36) is well-behaved at $\phi = 0$.

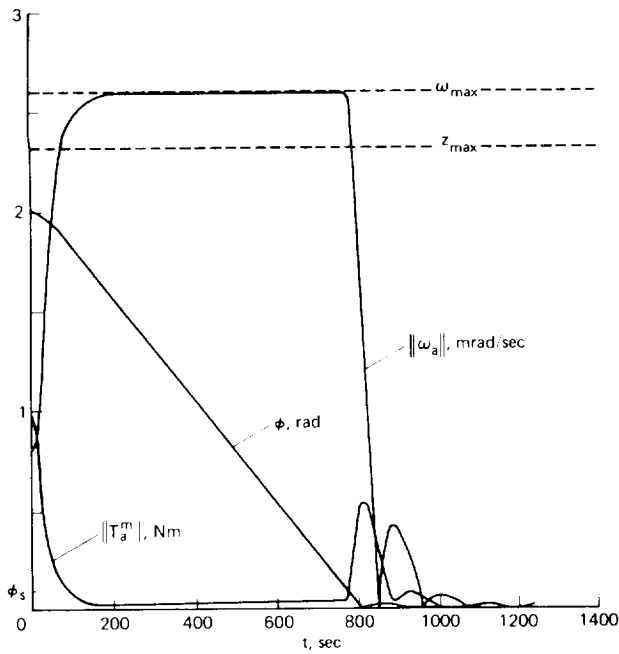


Figure 4.— A particular response of the system in example 8 in terms of magnitudes of torque, angular velocity and attitude error.

The response of the system to the initial condition, wheels locked prior to $t = 0$; $\phi(0) = 2$ (rad); $c^t(0) = -3^{1/2}(1,1,1)$; $\omega_a(0) = 0.5(1,-1,-1)$ (mrad/sec) is plotted in figures 4-6. These curves were obtained on a digital computer.

The response may be divided roughly into three parts. For $0 \leq t \leq 100$ seconds, the control generates pulselike torque to bring the spacecraft to its maximum angular velocity. For $100 \leq t \leq 750$ seconds, the vehicle coasts with maximum velocity toward the target; the small torques in this time interval probably counteract the gyroscopic term in equation (24). For $t \geq 750$ seconds, the control again generates pulselike torque to stop the spacecraft on target. At the end of the transient, the angular momentum of the system, which was initially in the main body, resides in the reaction wheels.

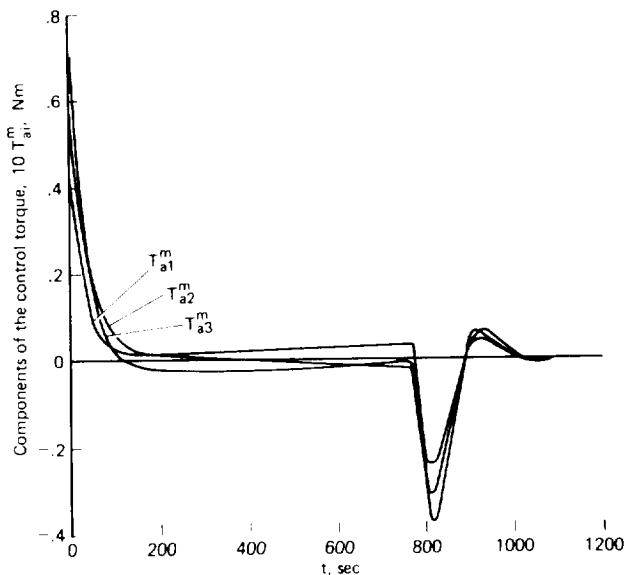


Figure 5.— The response of the system in example 8 in terms of the components of the control torque.

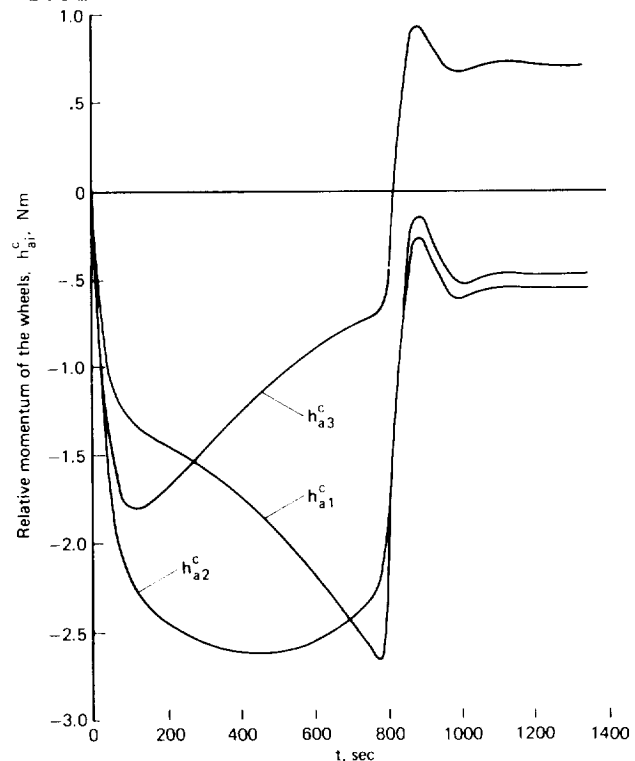


Figure 6.— The response of the system in example 8 in terms of the components of the relative momentum of the reaction wheels.

This system was, further, breadboarded on an airbearing platform using reaction wheels, motors, and star trackers (see ref. 8). This simulation showed the design to be practical. However, before the design can be considered to be complete, the following type of questions must be resolved. (1) How does the system respond to any admissible initial condition, and how well does it follow a moving target? (2) How significant is gyroscopic coupling? How sensitive is the system to (3) external torque disturbances, (4) variations in system parameters, and (5) changes in the form of the control law caused by partial failures in sensors and torquers? Such questions may be resolved by means of the techniques presented in the following sections.

GLOBAL ANALYSIS OF SYSTEM PERFORMANCE

Suppose now that a single-mode attitude control system has been designed. (See Applications, Case 2, for the discussion of a multimode design.) The problem is to determine whether the proposed design will perform adequately in all possible control situations. A control situation is defined by an initial condition, x_0 , and a pair of forcing functions, $\underline{u} = (\underline{u}_1, \underline{u}_2)$; x_0 is the state of the system at the time the control is initiated; \underline{u}_1 generates a motion of target attitude; and \underline{u}_2 generates a time history of disturbance. The latter may be due to external torque, or, as in a sensitivity analysis, it may represent variations in system parameters. The environment in which the system will operate is characterized by the set of admissible initial conditions θ_0 , perturbation functions n_1 and n_2 (see table 1) and the set of admissible forcing functions U . Every motion of the system, say \underline{x} , is the solution of the state equation $\dot{\underline{x}} = g[t, \underline{x}, \underline{u}(t)]$ for some x_0 in θ_0 , and some combined forcing function \underline{u} in U . That is, the state equation induces a transformation of the Cartesian product set $\theta_0 \times U$ onto the set X of all possible motions of the system. The elements of X will be denoted by $\underline{x} = x(t, x_0, \underline{u})$ for $t \geq 0$. Global analysis is concerned with the properties of this set X . The problem is to characterize X , and then to devise an effective procedure for computing the chosen characteristic.

Response Envelope

The primary purpose of an attitude control system is to maintain the spacecraft on target attitude. Hence, that property of X is of interest which characterizes the overall behavior of attitude error. To decide at any instant of time how near the actual attitude is to the desired attitude, it is necessary to have a notion of magnitude of attitude error. This may be introduced by means of the attitude error function $m(R)$ as discussed in the previous section. Although this function may be the same one that was used to design the control law, in general, it may be different. Each motion \underline{x} of the system generates a corresponding time history \underline{m} of the magnitude of attitude error. It is a positive scalar function of time which will be denoted by $m(t, x_0, \underline{u})$ for $t \geq 0$. Let M be the set of all such curves generated by X , or equivalently, by the set of all possible control situations $\theta_0 \times U$. The system response envelope, denoted by \underline{m}^{**} , will be defined as the

function of time which at each instant is the maximum of all values of \underline{m} in \underline{M} at that time; that is, for all $t \geq 0$,

$$m^{**}(t) = \max_{x_0 \in \theta_0} \left[\max_{\underline{u} \in \underline{U}} m(t, x_0, \underline{u}) \right] \quad (37)$$

Thus, the response envelope is a global property of the system. It indicates system responsiveness. For any admissible initial condition, target motion, and disturbance the attitude error at any time $t \geq 0$ will not be greater than $m^{**}(t)$.

State Space Interpretation of the Response Envelope

The response envelope can be given the following state space interpretation. Let θ and θ_0 be represented schematically as in figure 7. Since m is independent of ω_a , the surfaces of constant $m(R)$ are nested cylinders in θ . The motion starting at $x_0 \in \theta_0$ and forced by $\underline{u} \in \underline{U}$ is a trajectory in θ . The cylinder being crossed at time t determines the associated value of m at t .

The same initial state x_0 but a different forcing function \underline{u} will generate a different trajectory. Consider the bundle of all such trajectories emanating from x_0 and generated by \underline{U} . This bundle defines at each $t \geq 0$ a moving set of states that are reachable from x_0 at time t . Such a set is shown crosshatched in figure 7. The maximum cylinder intersecting this set at t gives the value of m corresponding to the inner maximization in equation (37). In figure 7 it is denoted by m_2 .

Now, consider the union of all such moving sets generated by all $x_0 \in \theta_0$. This union defines a moving cloud of points $\theta(t, \theta_0)$ shown schematically for $t = 0$ and $t = t_1$ in figure 8. Initially, the cloud coincides with θ_0 .

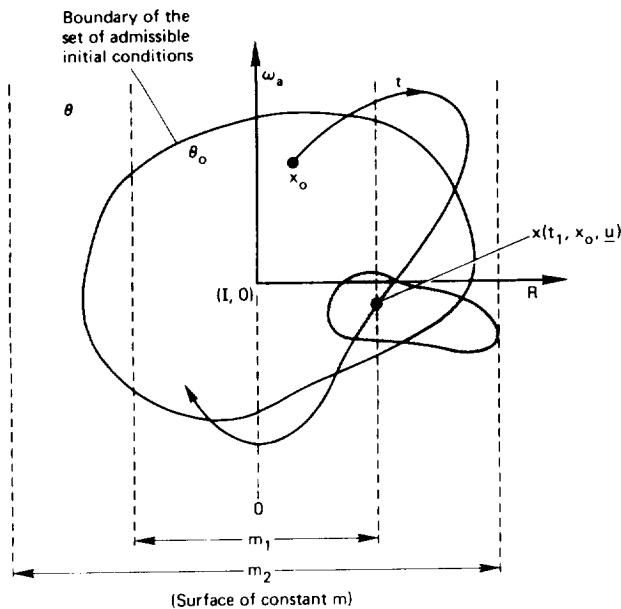


Figure 7.— Motion of set reachable from $x_0 \in \theta_0$.

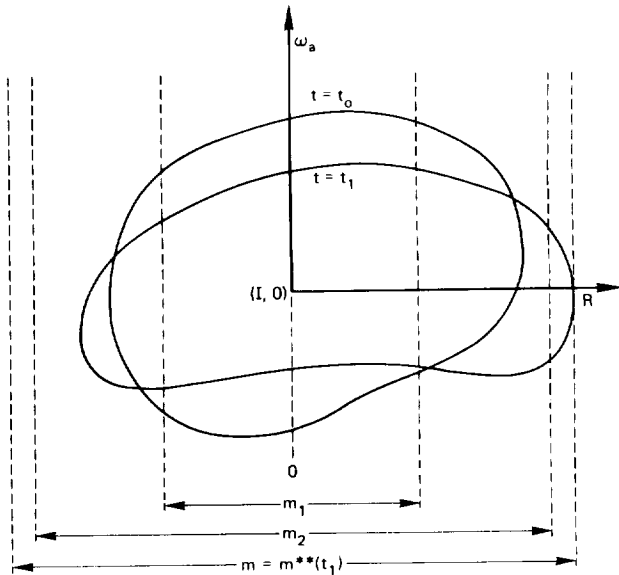
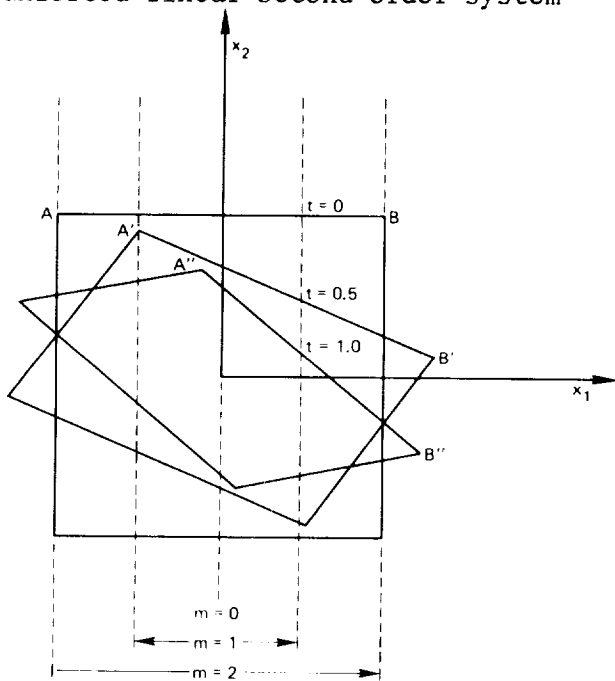


Figure 8.— Motion of cloud which is coincident with θ_0 at t_0 .

Thereafter it moves in response to system dynamics. At each $t \geq 0$ the maximum m -cylinder intersecting the cloud gives the value of the response envelope \underline{m}^{**} at that time. In other words, the knowledge of the motion of the boundary of the cloud is sufficient for the computation of the response envelope.

As an illustration of the preceding discussion consider the following unforced linear second-order system



$$\begin{pmatrix} \dot{x}_1 \\ \dot{x}_2 \end{pmatrix} = \begin{pmatrix} 0 & 1 \\ -1 & -1 \end{pmatrix} \begin{pmatrix} x_1 \\ x_2 \end{pmatrix}$$

with θ_0 being a square centered at the origin and bounded by $x_1 = \pm 1$, $x_2 = \pm 1$, and choose arbitrarily the error function $m(x) = |x_1|$. The corresponding motion of the cloud is sketched in figure 9. The corresponding response envelope is given in figure 10. In this simple case the response envelope is determined by the motion of vertices A and B.

Returning to the general case, consider the evolution of a piece of the boundary of the cloud, which at time t_1 is shown schematically as ABC in figure 11. At a later time t_2 it transforms into A'B'B'C', which is the envelope of all moving

Figure 9.— Motion of the cloud of states for the example.

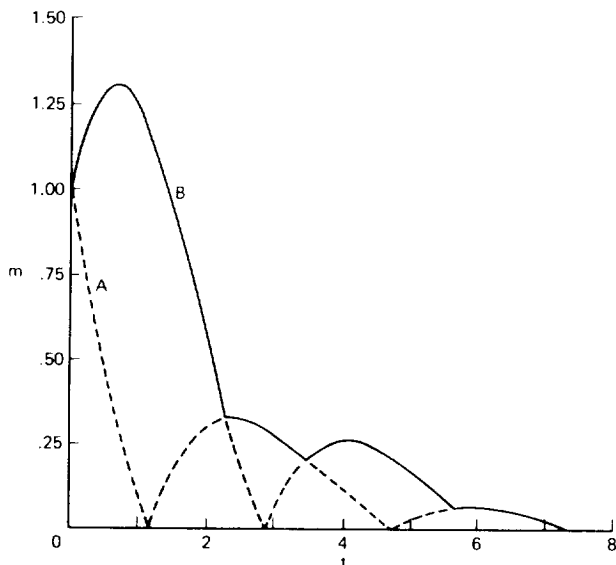


Figure 10.— Response envelope of system in example.

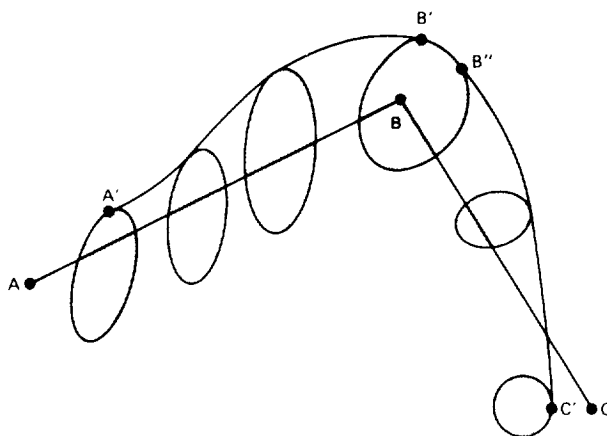


Figure 11.— The Huygen's construction of the boundary of cloud.

sets emanating from ABC. The image of ABC at some still later time t_3 is given by the envelope of all moving sets emanating from A'B'B''C', and so on for later times. It can be seen that this is the standard construction of wave fronts. Thus, for every initial condition x_0 on the boundary of θ_0 , there is a \underline{u} with values on the boundary of $U(t)$ for every $t \geq 0$, such that the resulting trajectory \underline{x} remains on the boundary of the moving cloud for $t \geq 0$. Note that the system was assumed to be in a fixed mode.

Suppose there is a function $V(t,x)$ such that $V(t,x) > 0$ outside, $V(t,x) = 0$ on the boundary, and $V(t,x) < 0$ inside the cloud. Consider the differentiable portions of the boundary and let $\dot{V}(t,x,u)$ denote the time rate of change of V along a trajectory. Note that since \dot{V} depends on trajectory, it depends on u . According to the preceding discussion, the boundary is characterized by two properties: (1) it is part of the cloud, that is, at each point on the boundary there is a $\underline{u} \in U$ such that $\dot{V}(t,x,u) = 0$, and (2) no trajectory can penetrate the boundary outward, that is, at each point on the boundary and every $\underline{u} \in U$, $\dot{V}(t,x,u) \leq 0$. Therefore, \dot{V} satisfies the following equation on the boundary

$$\max_{u \in U} \dot{V}(t,x,u) = 0 \quad (38)$$

But, $\dot{V} = V_t + V_x \dot{x}$, and $\dot{x} = g(t,x,u)$ where the subscripts indicate partial differentiation. Hence, equation (38) can be expressed as follows:

$$V_t + H(t,x,V_x) = 0 \quad (39)$$

where

$$H(t,x,V_x) = \max_{u \in U} V_x(t,x)g(t,x,u) \quad (40)$$

Thus, the differentiable portions of the boundary satisfy the Hamilton-Jacobi equation (39) with the boundary condition $\{x:V(0,x) \leq 0\} = \theta_0$. The corresponding response envelope is given for $t \geq 0$ by

$$m^{**}(t) = \max_{\{x:V(t,x) = 0\}} m(x) \quad (41)$$

That is, $m^{**}(t)$ is the maximum cylinder intersecting the cloud at t .

COMPUTATION OF RESPONSE ENVELOPES

According to the preceding discussion, the computation of a response envelope involves the solution of the Hamilton-Jacobi equation (39). The response envelope is given in terms of this solution by equation (41). Two methods for solving (39) are discussed in the present section. One, an

approximate method, is based on the Liapunov theory of stability. The other, an exact method, is based on the theory of optimal control.

Approximate Computation of Response Envelopes

Suppose $V^+(t,x) = 0$ is a smooth surface which at each $t \geq 0$ encloses the moving cloud without necessarily being its boundary; that is, suppose that for each $t \geq 0$,

$$\{x:V(t,x) \leq 0\} \subset \{x:V^+(t,x) \leq 0\}$$

Then property (1) of the exact boundary may be dropped with the result that V^+ satisfies the following inequality which is characteristic of Liapunov functions

$$V_t^+ + H(t,x,V_x^+) \leq 0 \quad (42)$$

This is the Hamilton-Jacobi equation with equality replaced by (\leq). The boundary condition is

$$\{x:V^+(0,x) \leq 0\} \supset \theta_0 \quad (43)$$

Equation (42) must hold for all $t \geq 0$, and all x in θ such that $V^+(t,x) = 0$.

It is very easy to construct solutions to (42). Simply, let

$$V^+(t,x) = V_1(t,x) - V_2(t) \quad (44)$$

where V_1 is such that for some finite a ,

$$\{x:V_1(0,x) \leq a\} \supset \theta_0 \quad (45)$$

and where V_2 is the solution of the following ordinary, first order, scalar differential equation with $V_2(0) = a$.

$$\dot{V}_2 = \max_{\{x \in \theta: V_1 = V_2\}} W \quad (46)$$

where

$$W = V_{1t} + H(t,x,V_{1x}) \quad (47)$$

Then V^+ so defined solves (42) as can be seen by direct substitution. The corresponding approximate response envelope is given by

$$m^+(t) = \max_{\{x \in \theta: V_1 = V_2\}} m(x) \quad (48)$$

By construction, $m^+(t) \geq m^{**}(t)$ for all $t \geq 0$. For this reason such an approximation will be called an upper estimate of the response envelope. Such an estimate is useful because it may serve as a basis for accepting a proposed design: under no circumstances can the attitude error be larger than $m^+(t)$ at any $t \geq 0$. Any function satisfying the boundary condition (45) may be used to compute an upper estimate. Of course, the fidelity with which m^+ represents m^{**} depends on the choice of V_1 . A poor choice will result in an overly pessimistic estimate of system performance. The following simple example illustrates the above discussion. The selection of V_1 for attitude control systems is discussed later (see eq. (51)).

Consider the second-order system

$$\begin{aligned} \dot{x}_1 &= -x_1 \\ \dot{x}_2 &= (2e^{-2t} - 2)x_2 + x_2 u \end{aligned}$$

where the forcing function $|u| \leq 1$. Suppose that the set of admissible initial conditions is the unit square, namely, $\theta_0 = \{x: |x_1| \leq 1, |x_2| \leq 1\}$, and that the error function $m = (x_1^2 + x_2^2)^{1/2}$. Let

$$V_1 = x_1^2 + x_2^2$$

Then condition (45) is satisfied for $a = 2$. The time derivative of V_1 along any trajectory is

$$\dot{V}_1 = -2x_1^2 + 2(2e^{-2t} - 2 + u)x_2^2$$

Hence,

$$W = -2x_1^2 + 2(2e^{-2t} - 1)x_2^2$$

and the maximum of W on the boundary $V_1 = V_2$ is $(4e^{-2t} - 2)V_2$. Therefore, the differential equation (46) is

$$\dot{V}_2 = (4e^{-2t} - 2)V_2$$

whose solution for $V_2(0) = 2$ is

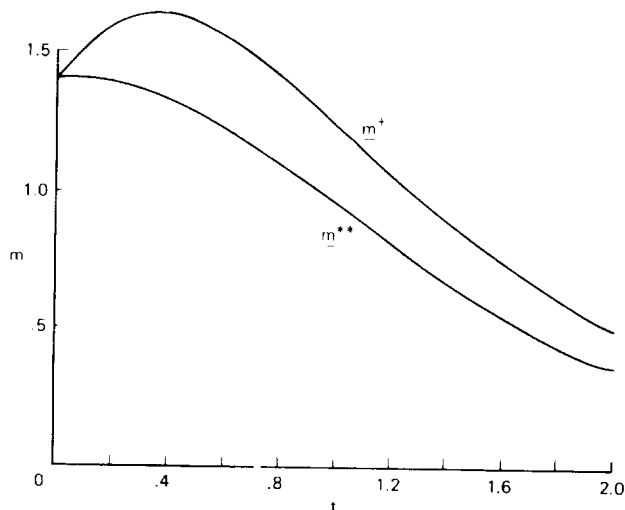
$$V_2(t) = 2e^{2(1-t-e^{-2t})}$$

So that the upper estimate is

$$m^+(t) = \sqrt{2} e^{(1-t-e^{-2t})}$$

On the other hand, in this simple example the exact response envelope can be obtained analytically as

$$m^{**}(t) = \left[e^{-2t} + e^{2(1-t-e^{-2t})} \right]^{1/2}$$



Both curves are shown in figure 12 for comparison. The difference between m^{**} and m^+ is due to the difference between the moving cloud and the approximating set $V_1 - V_2 \leq 0$. Thus, the cloud becomes squashed along x_1 ; while, the approximating set remains circular.

The calculations in the above example were sufficiently simple to be carried out by hand. For practical systems, these calculations will most likely have to be done on a computer. An outline of a possible computer program is given in table 2. It is assumed that V_1 and "a" satisfying (45) have been selected. The computation results in an

estimate \hat{m} of m^+ on the interval $0 \leq t \leq T$, for some chosen T . The estimate \hat{m} is assumed to be sufficiently accurate when a refinement of the grid G causes no significant changes in \hat{m} .

TABLE 2.- COMPUTATION OF UPPER ESTIMATES

Step 1.	Set $V_2(0) = a$
Step 2.	Cover the surface $V_1(t_k, x) = V_2(t_k)$ by a grid G .
Step 3.	Compute W from equation (47) and m from its defining equation, and maximize both over G , denoting the maximum of m by \hat{m} .
Step 4.	Step forward: $V_2(t_{k+1}) = V_2(t_k)W(t_k)\Delta t$.
Step 5.	Repeat steps 2 to 4 for all t_k in $[0, T]$. The result is an estimate \hat{m} of m^+ over $[0, T]$.

It may be noted that table 2 represents the computational procedure that is followed in a typical stability analysis by means of Liapunov functions. The only modification, aside from the maximization of m , is that here the

Liapunov conditions are tested at $V_1 = V_2$ with V_2 a computed function of time, rather than $V_1 = v_i$ for some preassigned collection of numbers $\{v_i\}$.

Exact Computation of the Response Envelope

Consider now the exact solution of the Hamilton-Jacobi equation (39). Suppose that $V(t,x)$ is differentiable for all x of interest and all $t \geq 0$. Let the trajectory $x(t) = x(t, x_0, u)$ lie on the boundary $V(t,x) = 0$, that is, $V[t, x(t)] = 0$ for all $t \geq 0$. Let $p(t)$ be the outer normal to the moving surface along $x(t)$, that is, $p(t) = V_x^t[t, x(t)]$ for all $t \geq 0$. The differential equation satisfied by p may be obtained as follows. Let $x^*(t) = x(t, x_0^*, u^*)$ be a neighboring trajectory, which also lies on the moving boundary, and let $\delta x(t) = x^*(t) - x(t)$. For sufficiently small δx , $V(t, x^*) = V(t, x) + p^t \delta x$. Hence, $p^t \delta x(t) = 0$, for all $t \geq 0$. Consequently,

$$\dot{p}^t \delta x + p^t (\delta x)' = 0$$

But the system state equation is $\dot{x} = g(t, x, u)$. Hence,

$$(\delta x)' = g_x(t) \delta x + g_u(t) \delta u$$

where the coefficient matrices are evaluated along $x(t)$, and $u(t)$, and δu is such that $p^t g_u \delta u = 0$ because the neighboring trajectory x^* is also on the moving boundary. Therefore,

$$[\dot{p}^t + p^t g_x(t)] \delta x = 0$$

since δx is an arbitrary vector in the tangent space of $V(t,x) = 0$ at x , $\dot{p} + g_x^t p = kp$ for any scalar k . Choosing $k = 0$, one obtains the following differential equation for the normal p

$$\dot{p} = -g_x^t(t)p$$

Thus, the motion of a planar element which is given at $t = 0$ by position x_0 and normal p_0 satisfying $V(0, x_0) = 0$ and $p_0 = V_x^t(0, x_0)$, respectively, satisfies the following standard equations of optimal control, which are derived rigorously in reference 9:

$$\dot{x} = g(t, x, u) \tag{49a}$$

$$\dot{p} = -g_x^t(t, x, u)p \tag{49b}$$

$$u = \operatorname{argmax}_{u \in U} H(t, x, p) \tag{49c}$$

where $H = p^t g(t, x, u)$. Equation (49c) expresses the Huygen's construction (fig. 12) of the boundary. The time history of attitude error \underline{m}^* corresponding to this planar element is thus a function of only x_0 on the initial boundary. For each $t \geq 0$ the response envelope is given by

$$m^{**}(t) = \max_{\{x_0: V(0, x_0) = 0\}} m^*(t, x_0) \quad (50)$$

This computational procedure is outlined in table 3. It is assumed that $\theta_0 = \{x: V(0, x) \leq 0\}$, that $V(0, x)$ is given, and that it is smooth. The estimate is assumed to be sufficiently accurate when a refinement of the grid G causes no significant change in \hat{m} . Pontryagin's maximum principle (ref. 9) guarantees that \hat{m} will converge to the exact response envelope \underline{m}^{**} with grid refinement if equations (49) have unique solutions for given initial conditions. This will be the case if, for example, in table 1, g is differentiable, perturbation functions n_1 and n_2 are smooth and have maximal rank almost everywhere, f in the dynamic equation is invertible with respect to y_2 , and $U = \{u: \|u\| \leq 1\}$.

TABLE 3.- COMPUTATION OF THE RESPONSE ENVELOPE

Step 1.	Cover the initial surface $V(0, x) = 0$ by a grid G .
Step 2.	Set $\hat{m} = 0$ on the time interval $[0, T]$.
Step 3.	Set initial conditions $(x, p) = [x_i, V_x^t(0, x_i)]$ for $i \in G$.
Step 4.	Solve the canonical equations (49) storing $\max[m_i^*(t), \hat{m}(t)]$.
Step 5.	Repeat steps 3 and 4 until G is exhausted. The resulting \hat{m} is an estimate of \underline{m}^{**} on the computation interval.

It may be noted that this computation of the response envelope is essentially no more complicated than the maximization of $m(T)$ for a single initial condition x_0 . In the latter case all directions of initial p must be tested. This is equivalent to θ_0 being an infinitesimal sphere about the initial state x_0 .

The main advantages of the computation outlined in table 3 are that there is no need to guess a Liapunov function, and that, at least in the limit, the exact response envelope is being computed. On the other hand, the computation outlined in table 2 does not require repetitive solution of the system state equation or its adjoint. Hence, the conditions on the state equation are much weaker. Of course, there is also the advantage that in certain nontrivial cases the required computation can be carried out by hand.

If the computer is to be used, the computation time required is of practical interest. This can be estimated by assuming that the set of admissible initial conditions θ_0 is a sphere. Assuming that there are N_x subdivisions of each coordinate interval, there are $N_G = 2nN_x^{n-1}$ grid points in G . This is the number of computations involved in step 3 of table 2. Assuming that there are N_t points along the time interval, the total number of computations is $N = 2nN_x^{n-1}N_t$. On the other hand, in table 3 there are N_G time histories, each requiring N_t computations. Thus, in either case there are $N = 2nN_x^{n-1}N_t$ computations. For example, if $N_x = 10$, $N_t = 100$, then $N = 1.2 \times 10^8$ if $n = 6$, and $N = 6 \times 10^4$ if $n = 3$. Assuming 100 microseconds per computation, the computation time is of the order of 3 hours for $n = 6$, and only 10 seconds for $n = 3$. The large reduction in computation time accompanying the reduction in the dimension of the state space motivates the following discussion of comparison models. It will be seen that the performance of an attitude control system can be compared with that of a spherically symmetric model whose state space is essentially three-dimensional.

Comparison Models for Attitude Control Systems

From the practical point of view, it is very desirable to be able to trade accuracy for reduced computer time in a meaningful way. A useful approximation to the response envelope is an upper estimate \underline{m}^+ such that for all $t \geq 0$,

$$m^+(t) \geq m^{**}(t)$$

As noted previously, such an estimate may be used as a basis for accepting a proposed design: for no combination of possible initial condition, target motion, and disturbance will the magnitude of attitude error be greater than indicated by the upper estimate. Such an estimate may be computed using a comparison model having two properties. First, the comparison model must be sufficiently simple that the computation of its response envelope is practical. Second, it must be known analytically that this response envelope is an upper estimate on the response envelope of the given system. A way for constructing comparison models will now be discussed.

Suppose that two initial states x_1 and x_2 happen to be such that for every admissible forcing function \underline{u}^1 there is an admissible forcing function \underline{u}^2 such that for all $t \geq 0$,

$$m(t, x_1, \underline{u}^1) = m(t, x_2, \underline{u}^2)$$

and conversely. Then one may consider the two states to be equivalent for the computation of the response envelope. It would be a waste of computer time to include both states in the grid G . For efficient use of the computer, the grid should consist of only the representative states, each representing its equivalence class. For example, suppose that the state space is n -dimensional, that the state equation is

$$\dot{x} = -x + u$$

that the set of admissible initial conditions is

$$\theta_0 = \{x: x^t x - 2 \leq 0\}$$

that for all $t \geq 0$,

$$U = \{u: \|u\| \leq 1\}$$

and that the magnitude function is

$$m(x) = \|x\|$$

Then it is sufficient to include only one point in G , say $x^t = (\sqrt{2}, 0, \dots, 0)$.

This simple example suggests that the concept of state equivalence is potentially useful for speeding the computation of response envelopes. Its actual usefulness depends on the ease with which equivalence can be determined. The equivalence of two states can always be determined during the computation of the response envelope. Of course, this is not very helpful. Efficiency is achieved only if equivalence is determined before the computation is initiated. It seems that for an arbitrary system such an a priori determination of equivalence is difficult. But, consider the situation from the other end. That is, start by choosing a partition of the state space, and construct a model whose set of equivalence classes coincides with this partition. Then adjust this model so that the set \underline{X}^C of its possible motions includes the set \underline{X} of all possible motions of the given system. Then the response envelope of the model can be computed efficiently, and it will be an upper estimate of the response envelope of the given system. The desired trade-off between computer time and accuracy is thus accomplished. A fine partition will result in small saving of time, but the estimate will be close to the response envelope of the given system. In fact, for the finest partition, namely identity, no time is saved, and no error is made. As the partition is made coarser, equivalence classes become larger, computation time smaller, and the estimate more conservative. Of course, if the comparison model happens to be the exact model of the given system, time is saved without loss in accuracy.

A convenient way to define a partition is by means of a group of transformations. In that case two states x_1 and x_2 are equivalent if there is a transformation taking x_1 into x_2 . A partition is obtained because a group has an identity (reflexivity), an inverse (symmetry), and closure (transitivity).

In summary, a comparison model may be constructed for a given system as follows. Based on physical insight, choose a group of transformations. The choice defines a partition on the state space. Construct a model whose equivalence classes give this partition. Adjust the model so that the set of its motions \underline{X}^C includes all possible motions of the given system. The result is a comparison model of the given system.

Now consider a comparison model for attitude control systems. The system state x can be represented by (ϵ, ω_a) where ϵ is the Euler vector

defined by equation (19b) and ω_a is body angular velocity. Then, x can be considered either as one 6-dimensional vector, or as a pair of 3-dimensional vectors. Consider the set of transformations τ with elements τ_A , where for each rotation matrix A ,

$$\tau_A(x) = (A\varepsilon, A\omega_a)$$

τ is a group. Two states $x_1 = (\varepsilon_1, \omega_{a1})$ and $x_2 = (\varepsilon_2, \omega_{a2})$ are equivalent if the triangle formed by ε_1 and ω_{a1} is congruent to the triangle formed by ε_2 and ω_{a2} . Hence, the only properties of the initial state that matter in the computation of the response envelope are the length of ε , the length of ω_a , and the angle between these two vectors. Comparison models generated from τ will be called spherically symmetric. One such model is given in table 4.

TABLE 4.- MODEL OF SPHERICALLY SYMMETRIC SYSTEMS

State space	$X = E^6, \quad x = (\varepsilon, \omega_a)$
Region of operation	$\theta = \{x: \ \varepsilon\ < 2\}$
Admissible initial conditions	$\theta_0 = \{x: \ \varepsilon\ ^2 + v_1\ \omega_a\ ^2 \leq v_2 < 4\}$
State equation	
Kinematic equation	$\dot{\varepsilon} = \frac{1}{2} S(\omega_a + y_1)\varepsilon + \frac{1}{2} \eta(\omega_a + y_1)$
Dynamic equation	$\dot{\omega}_a = -[f(\ \varepsilon\)a_1\varepsilon + a_4\omega_a] + y_2$
Perturbation	
Target velocity	$y_1 = a_5 u_1(t)$
Disturbance	$y_2 = f(\ \varepsilon\)[-a_2\varepsilon u_0(t) + a_3 S(\varepsilon)u_2(t)]$
Admissible forcing functions	$\ u_1(t)\ ^2 + u_0(t) ^2 + \ u_2(t)\ ^2 \leq 1, \text{ for all } t \geq 0$
Magnitude of attitude error	$m(x) = \phi$

The state space is six-dimensional. The state is represented by the Euler vector ε and body angular velocity ω_a . Points with $\|\varepsilon\| = 2$ are excluded from the region of operation θ because the kinematic equation (20b) is singular there. The set of admissible initial conditions θ_0 is an ellipsoid whose shape and size are determined by constant scalars v_1 and v_2 . The angular acceleration is a sum of the nominal control law and a perturbation. The nominal control law is a weighted sum of the Euler vector and angular velocity. The perturbation consists of two terms: one acts parallel to ε ; the other acts perpendicular to ε . The forcing vector u is seven-dimensional. Three components u_1 are used to generate target velocity; one component u_0 is used to generate perturbation parallel to ε ; and three components u_2 are used to generate perturbations perpendicular to ε . The combined forcing vector is spherically bounded by 1. The intensity of perturbations is determined by the constant scalars a_2, a_3 , and a_5 which are

assumed to be greater than zero. The magnitude of attitude error is the error angle ϕ . When the spacecraft is on target, $\phi = 0$; otherwise it is between 0 and π .

That this model is spherically symmetric can be seen by considering the effect of any τ_A from τ . Thus, $\tau_A(\theta) = \theta$, and $\tau_A(\theta_0) = \theta_0$. The kinematic equation is spherically symmetric because

$$\begin{aligned} (A\epsilon) \dot{} &= \\ A\dot{\epsilon} &= \frac{1}{2} AS(\omega_a + y_1)A^t A\epsilon + \frac{1}{2} \eta A(\omega_a + y_1) \\ &= \frac{1}{2} S[(A\omega_a) + (Ay_1)](A\epsilon) + \frac{1}{2} \eta [(A\omega_a) + (Ay_1)] \end{aligned}$$

and $\|Ay_1\| = \|y_1\| = a_5\|u_1\|$. Spherical symmetry of the dynamic equation can be shown similarly. Finally, $\phi(ARA^t) = \phi(R)$ because the trace is an invariant under a rotation transformation. So, for any two initial states on the boundary of θ_0 , say x_1 and x_2 , if there is a rotation matrix A such that $x_2 = \tau_A(x_1)$, then for any \underline{u}^1 there is a \underline{u}^2 such that for all $t \geq 0$,

$$\phi(t, x_1, \underline{u}^1) = \phi(t, x_2, \underline{u}^2)$$

Consequently, the model is spherically symmetric, and the grid G in either table 2 or table 3 may consist of only representative states of the form $x = (\epsilon, \omega_a)$ where

$$\epsilon = (v_2 - v_1 w^2)^{1/2} \begin{pmatrix} 1 \\ 0 \\ 0 \end{pmatrix}, \quad \omega_a = w \begin{pmatrix} \cos \psi \\ \sin \psi \\ 0 \end{pmatrix}$$

$$0 \leq w \leq \left(\frac{v_2}{v_1}\right)^{1/2}$$

$$0 \leq \psi \leq \pi$$

Thus, the computation of the system response envelope requires a maximization over only two parameters, w and ψ . This is practical.

The parameters a_i in table 4 were assumed constant in order to simplify discussion. It is clear that these parameters may be allowed to be functions of $\|\epsilon\|$, $\|\omega_a\|$, and $\epsilon^t \omega_a$ as well as time. In addition, perturbations along ω_a and perpendicular to it may be included. Thus, the condition of spherical symmetry is not so restrictive as might appear from table 4. If the given system is spherically symmetric, then the recognition of this fact can greatly speed the computation of its response envelope. If the given system is not spherically symmetric, then it can be represented by a spherically symmetric

model by absorbing the asymmetry into perturbations. Then the response envelope of the comparison model will be an upper estimate of the response envelope of the given system (see example 10).

In the computation of upper estimates by means of Liapunov functions as outlined in table 2, it is necessary to give a V_1 function. One such function found to be useful in practice is given by the following equation:

$$v_1(x) = \int_0^\phi g_1(\phi) d\phi + 2a_4 \left(1 - \cos \frac{1}{2} \phi\right) + \frac{1}{2a_1} \|\omega_a\|^2 + \frac{1}{2} \epsilon^t \omega_a \quad (51)$$

where $g(\phi) = f[2 \sin(1/2)\phi]/[2 \sin(1/2)\phi]$, and f is the function appearing in the dynamic equation in table 4. It may be noted that this V_1 is spherically symmetric: for any rotation matrix A , $V_1[\tau_A(x)] = V_1(x)$. Its form may be thought of as a natural extension to three axes of the Liapunov function commonly used in the analysis of single axis servos. Thus, the first two terms on the right of equation (51) depend only on the magnitude of attitude error. The next term depends only on the magnitude of angular velocity. The last term represents coupling, which depends on these magnitudes and on the angle between the error axis and the angular velocity vector.

Applications

The following two examples illustrate the use of spherically symmetric models for the computation of response envelopes by means of procedures outlined in tables 2 and 3.

Example 9- This example illustrates the computation of upper estimates of response envelopes by means of Liapunov functions (table 2). Consider the system discussed in example 8, page 20. The nominal control law is given by equation (36). It is spherically symmetric. The time history of the error angle corresponding to a particular control situation is shown in figure 4. Now global behavior of this system will be considered.

To simplify the discussion, let the system be normalized as follows: time $t \rightarrow t/\omega_{amax}$; angular velocity $\omega_a \rightarrow \omega_a \cdot \omega_{amax}$. Then the dynamic equation in the absence of perturbation is

$$\dot{\omega}_a = -\frac{1}{\phi_s} \text{sat}(\phi, \phi_s) c - \frac{1}{\phi_s} \omega_a \quad (52)$$

The following upper estimates were computed using the Liapunov function,

$$V_1(x) = \int_0^\phi \text{sat}(\phi, \phi_s) d\phi + \frac{2}{\phi_s} \left(1 - \cos \frac{\phi}{2}\right) + \frac{1}{2} \phi_s \|\omega_a\|^2 + \sin\left(\frac{\phi}{2}\right) c^t \omega_a \quad (53)$$

which is a special case of equation (51).

Case 1 - single-mode nominal system- For this case the set of admissible initial conditions is assumed to be given by

$$\theta_0 = \{x: \phi \leq 2, \|\omega_a\| \leq 1\} \quad (54)$$

It is also assumed that the dynamic equation is unperturbed (i.e., total angular momentum $h_s = 0$ for all $t \geq 0$) and that the angular velocity of the target is spherically bounded by a fraction b of the maximum angular velocity allowed for the spacecraft (i.e., $\|\omega_d\| \leq b\omega_{amax}$, for $t \geq 0$). The results are given in figure 13. Note from (52) and (54) that since $\|\omega_a\|' < 0$ for $\|\omega_a\| > 1$, points with $\|\omega_a\| > 1$ may be excluded from step 2, table 2. That

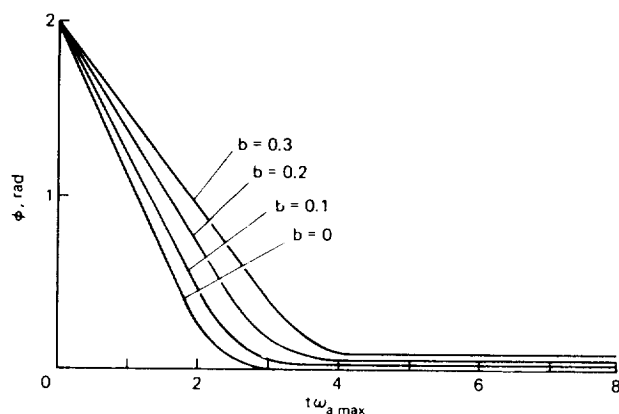


Figure 13.- Global response of nominal single-mode system for several bounds on target angular velocity.

is, one needs to consider only that part of the Liapunov surface which is inside the cylinder $\|\omega_a\| \leq 1$. The curve $b = 0$ indicates the responsiveness of the nominal system to step changes in target attitude. Thus, for any admissible initial condition, the attitude error will not be greater than the value indicated by this curve. It can be seen that the system is not only asymptotically stable on θ_0 , but it is essentially on target ($\phi \leq 0.01$ rad) no later than $3/\omega_{amax} = 1150$ seconds after the initiation of control. Curves with $b > 0$ indicate how well the system follows a time varying target. Thus, the curve $b = 0.2$, for example, shows that for any admissible initial condition and any target motion with

angular velocity bounded by $0.2\omega_{amax} = 0.322$ mrad/sec, the attitude error will not be greater than indicated by this curve. It is emphasized that a curve in figure 13 is not the response to a particular control situation. Rather, it is a global description of system behavior under all possible (there are infinitely many) control situations.

Case 2 - multiple-mode nominal system- In this case the set of admissible initial conditions is assumed to be given by

$$\theta_0 = \{x: \phi \leq \pi, \|\omega_a\| \leq 1\} \quad (55)$$

It may be noted that this set includes points at which the error axis c is double valued, so that the control (52) is undefined there. However, the system may be controlled using three modes as follows. For a fixed δ choose an "a" so that the maximum of ϕ on the set

$$\theta_1 = \{x: V_1(x) \leq a, \|\omega_a\| \leq 1\} \quad (56)$$

is $\pi - \delta$, and let the maximum of ϕ on $\theta_1 \cap \{\|\omega_a\| = 0\}$ be denoted by ϕ_m . If $x(0)$ is in θ_1 , let the system be controlled by (52). Otherwise, apply maximum angular acceleration antiparallel to $\omega_a(0)$ until either θ_1 is entered or $\omega_a = 0$. This mode lasts for at most $\|\omega_a(0)\|/\dot{\omega}_{amax}$ seconds. If θ_1 is entered, let the system be controlled by (52). Otherwise, offset the error attitude R by $\Delta\phi = \pi - \phi_m$ by introducing a fictitious change in target attitude. This brings x into θ_1 where the system can be controlled by (52) while the offset is removed with angular velocity which is bounded by, say, $b_1\omega_{amax}$. The effective target velocity in this mode is bounded by $(b + b_1)\omega_{amax}$. The offset will be removed after $(\pi - \phi_m)/(b_1\omega_{amax})$ seconds. Thereafter, the angular velocity is spherically bounded by $b\omega_{amax}$, as in case 1. The plots (fig. 14) show the behavior of the resulting system with $\epsilon = 0.01$, $b_1 = 0.1$, and $\omega_{amax} = 2/\phi_S = 20$ rad/sec². Note that curve $b = 0$ shows the regulator is asymptotically stable for all attitude errors.

Case 3 - perturbations in the dynamic equation- In this case it is assumed that the dynamic equation is given by

$$\dot{\omega}_a = -\frac{1}{\phi_S} \text{sat}(\phi, \phi_S)c - \frac{1}{\phi_S} \omega_a + y_2$$

where the first two terms correspond to the nominal control law (52) and y_2 is the perturbation. The set of admissible initial conditions is assumed to be given by (55), and the target attitude is assumed to be stationary.

Figure 15 shows upper estimates due to perturbation of the form

$$y_2 = b \left(\frac{h_{max}}{j_{min} \omega_{amax}} \right) S(\omega_a) u_2$$

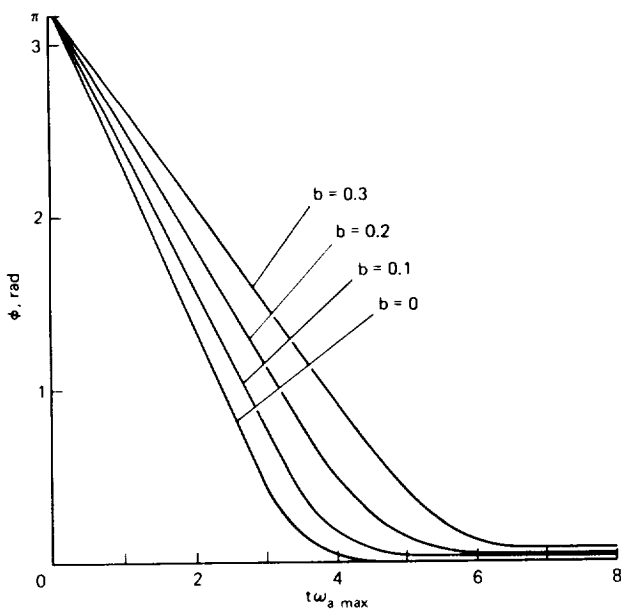


Figure 14.— Global response of nominal multimode system for several bounds on target angular velocity.

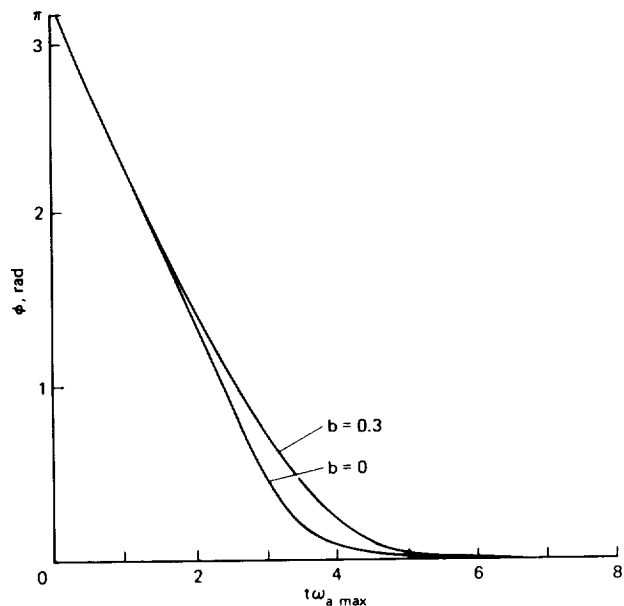


Figure 15.— Sensitivity to gyroscopic coupling.

This perturbation is a (normalized) symmetric approximation of the gyroscopic term in equation (24) with $\|h_s\| \leq bh_{\max}$. The curve $b = 0.3$ shows that for the case considered (i.e., 0A0), gyroscopic coupling is not very significant even when the system is loaded with as much as 30 percent of its angular momentum storage capacity.

Figure 16 shows the performance of the system with an angular momentum dumping scheme (see example 3, p. 13). It is assumed that the total external torque is spherically bounded by $0.1T_{\max}$, and that the dumping scheme maintains the total angular momentum of the system spherically bounded by $0.3h_{\max}$.

Figure 17 shows the sensitivity of the system to spherical errors in commanded acceleration. The perturbation is assumed to be given by

$$y_2 = b [\| \text{sat}(\phi, \phi_s) c + \omega_a \| / \phi_s] u_2$$

From this figure one may conclude that spherical errors of the order of 10 percent affect the performance little. This means, for example, that 10 percent changes in moment of inertia, motor and power amplifier gains, or a misalignment of the motor-wheel pairs with respect to the body axes of about 3° is not detrimental to system performance. Even when such errors are large enough to cause 30 percent error in acceleration, the system remains asymptotically stable. If the system were controlled by means of control moment gyros, the plots in figure 17 would indicate system sensitivity to partial failures in the gyro package. The corresponding b may be taken to be (see example 2, p. 13)

$$b = \max_Q \| I - J_a^{-1} h_q(q) F(q) J_a \|$$

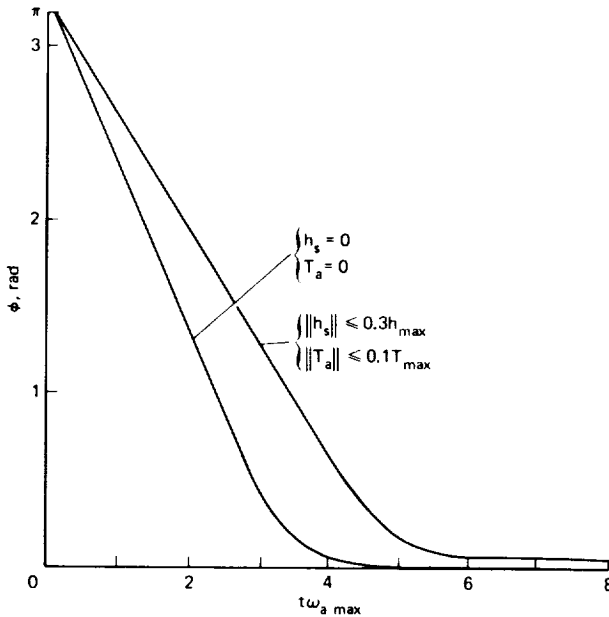


Figure 16.— Sensitivity to gyroscopic coupling and external torque.

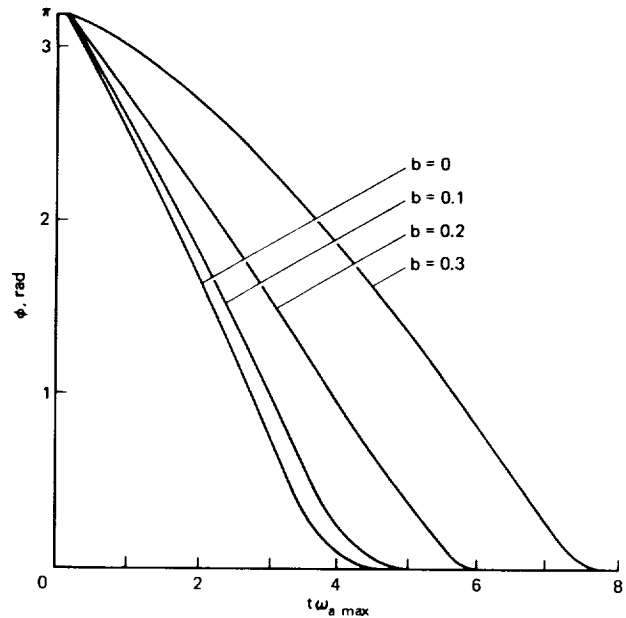


Figure 17.— Sensitivity to spherical errors in acceleration.

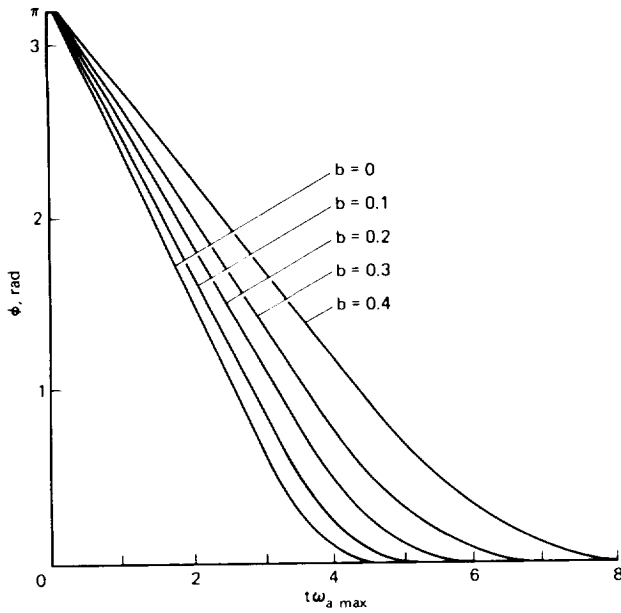


Figure 18.— Sensitivity to spherical errors in attitude error feedback.

Figure 18 shows the effects of spherical errors in attitude error feedback. The perturbation is assumed to be given by

$$y_2 = b[\text{sat}(\phi, \phi_S)/\phi_S]u_2$$

The plots in this figure may be used to determine system sensitivity to errors and partial failures in the attitude sensor.

Example 10— This example illustrates the use of spherically symmetric models and the procedure outlined in table 3 to compute upper estimates of response envelopes for systems which are not spherically symmetric.

Consider the system discussed in example 7 (p. 18). Spacecraft attitude is measured with star trackers, and the difference between the actual and commanded gimbal angles is used for attitude error feedback. Let the control law be given by equation (35) in which the functions g_i represent hard saturation. In addition, let the terms in the gain matrix involving the tangents of inner gimbal angles be set to zero, and let the multiplication by this matrix be followed by another hard saturation of each component. The resulting attitude error feedback is shown schematically in figure 19. Thus, the gimbal angle errors are clipped at 0.1 rad, passed through a gain matrix which is a function of the outer gimbal angles, and then again clipped. The result $g(R)$ is the attitude error feedback. The dynamic equation is assumed to be the following linear combination of $g(R)$ and body angular velocity ω_a

$$\dot{\omega}_a = -10g(R) - 10\omega_a$$

The problem is to determine the behavior of the system on the set of admissible initial conditions given by

$$\theta_0 = \{x: \|\epsilon\|^2 + \|\omega_a\|^2 \leq 1\}$$

The feedback $g(R)$ is highly nonlinear, and it is not spherically symmetric. However, it can be represented by a spherically symmetric, smooth function with perturbations. Thus, in the range $0 \leq \phi \leq 1$ rad,

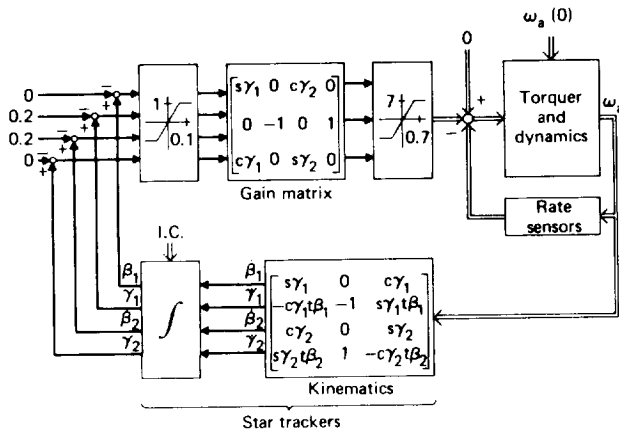


Figure 19.— Attitude error feedback used in example.

$$g(R) = -10[1 + (10\|\epsilon\|)^2]^{-1/2} [\epsilon + 0.55\epsilon u_0 - 2.5S(\epsilon)u_2]$$

with $u_0^2 + \|u_2\|^2 \leq 1$. (This representation was determined on a digital computer.) Hence, in table 4, $v_1 = v_2 = 1$, $f = 10[1 + (10\|\epsilon\|)^2]^{-1/2}$, $a_1 = 1$, $a_2 = 5.5$, $a_3 = 25$, and $a_4 = 10$. Figure 20 shows the corresponding response

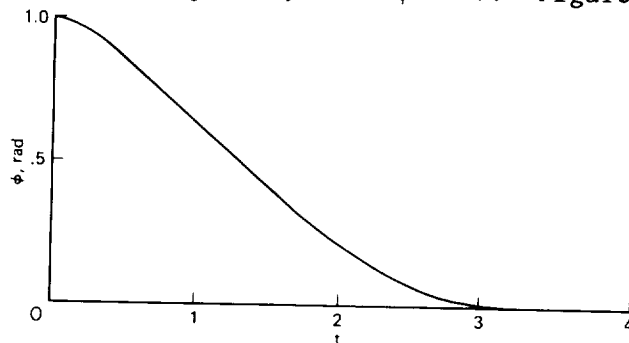


Figure 20.— Global response of the system.

envelope computed by means of the procedure outlined in table 3. (Eq. (49c) was made nonsingular almost everywhere by setting $a_5 = 0.001$ and requiring that $\|u_1\|^2 + u_0^2 + \|u_2\|^2 \leq 1$.) As can be seen from the figure, the system is asymptotically stable on θ_0 , and it is essentially on target after three units of time for any admissible initial condition.

CONCLUDING REMARKS

An approach to the design and global analysis of three-axis, large angle attitude control systems has been presented. The approach is general in the sense that it is not based on special properties of particular system components, but, rather, on properties common to all attitude control systems. By making use of the well-known properties of three-dimensional rotations, it was possible to apply the general techniques of control system theory to develop a practical design and analysis procedure for such systems. Attitude error, a kinematic equation, and a dynamic equation were formulated in a way that is convenient for the study of attitude control systems, and were collected in a general mathematical model of such systems. The notion of distance in attitude between spacecraft and target was introduced by means of attitude error functions. It was shown that such functions may be used to generate asymptotically stable control laws. In addition, such functions may be used to characterize the overall system behavior by means of response envelopes.

A state space interpretation of the response envelope was given, and the similarity between Liapunov's second method and optimal control theory was noted. Two procedures for computing the response envelope were presented. One, based on Liapunov's method, is approximate and gives upper estimates on the response envelope. The primary advantage of this procedure is that few continuity requirements are imposed on the system. The disadvantage is that there is no direct way to construct Liapunov functions. The second procedure, based on the theory of optimal control, is exact and direct, but it imposes more conditions on system dynamics.

The computation time required by either procedure depends on the dimension of the state space. The concept of spherically symmetric comparison

models was introduced as a means for reducing the effective dimension of the state space from 6 to 3. This reduction results in a large saving of computer time. Any attitude control system with six-dimensional space can be compared with a spherically symmetric model by absorbing the asymmetry into perturbations. Of course, if the given system is strongly asymmetric, the upper estimate obtained will be overly conservative.

The examples included in the report suggest that the proposed design and analysis technique is useful.

Ames Research Center
National Aeronautics and Space Administration
Moffett Field, Calif., 94035, October 20, 1970

APPENDIX A

METRIC PROPERTIES OF THE ϕ FUNCTION

The ϕ -function is defined for any rotation matrix R by

$$\phi(R) = \underset{[0, \pi]}{\text{arc cos}} \left\{ \frac{1}{2} [\text{trace}(R) - 1] \right\}$$

R may be interpreted as a rotation from d -basis into a -basis. Consider all paths from I to R . Each satisfies the differential equation

$$\dot{R} = S[\omega(t)]R$$

for some piecewise continuous $\underline{\omega}$. In addition, $R(0) = I$ and $R(t_f) = R$ for some fixed t_f . It will now be shown that for all such $\underline{\omega}$,

$$\phi(R) \leq \int_0^{t_f} \|\omega(t)\| dt \quad (A1)$$

The Hamiltonian is

$$H = \text{trace}[P^t S(\omega) R] + p_0 \|\omega\|$$

and the adjoint equation is

$$\begin{aligned} \dot{p}_0 &= 0 \\ \dot{P} &= S[\omega(t)]P \end{aligned}$$

Thus, for any $\underline{\omega}$, R and P have the same transition matrix $\phi(t)$. That is, $R(t) = \phi(t)$, and $P(t) = \phi(t)P_0$. Hence, for $0 \leq t \leq t_f$

$$\begin{aligned} \text{trace}[P^t S(\omega) R] &= \text{trace} [P_0^t \phi^t S(\omega) \phi] \\ &= \text{trace}[P_0^t S(\phi^t \omega)] \\ &= 2\omega^t \phi k \end{aligned}$$

where k is a constant. Therefore,

$$H = 2\omega^t \phi k + p_0 \|\omega\|$$

and the optimum ω is colinear with ϕk , that is colinear with $R(t)k$. But this means that the direction of ω is fixed in the d -basis. Therefore, $\omega(t)$ is at each t the eigenvector of $R(t)$, and the conclusion (A1) follows.

The second property of ϕ is the following. For any rotation matrices A and B ,

$$\phi(AB^t) \leq \phi(A) + \phi(B) \quad (A2)$$

Suppose the contrary, and denote AB^t by C and B by D^t . Then it would be true that $\phi(C) > \phi(D) + \phi(CD^t)$. That is, the angle of the composite rotation: from I to D , followed D to C , is smaller than the angle of direct rotation from I to C . This, according to (A1) is impossible. Hence (A2) is true.

Finally, consider the set of all rotation matrices. For any A and B in this set define

$$\phi(B,A) = \phi(AB^t) \quad (A3)$$

The function $\phi(B,A)$ so defined is a metric on the space of three-dimensional rotations. Indeed, (i) $\phi(B,A)$ is positive; (ii) $\phi(B,A) = 0$ if and only if $A = B$; (iii) $\phi(A,B) = \phi(B,A)$; (iv) $\phi(B,A) + \phi(A,C) \geq \phi(B,C)$. The triangle inequality holds because

$$\phi(B,C) = \phi(CB^t) = \phi[CA^t(BA^t)^t] \leq \phi(CA^t) + \phi(BA^t) = \phi(A,C) + \phi(B,A)$$

APPENDIX B

KINEMATIC EQUATION IN TERMS OF THE (ϕ, c) PARAMETERS

From equation (16) it follows that

$$-\sin \phi \dot{\phi} = \frac{1}{2} \text{trace} (\dot{R})$$

But, according to (13), $\dot{R} = S(\omega)R$. In addition, for any y in E^3 and any 3×3 matrix $A = (a_{ij})$,

$$\text{trace}[S(y)A] = -y^t \begin{pmatrix} a_{23} - a_{32} \\ a_{31} - a_{13} \\ a_{12} - a_{21} \end{pmatrix}$$

as can be checked by expanding both sides. Hence,

$$-\sin \phi \dot{\phi} = -\frac{1}{2} \omega^t \begin{pmatrix} r_{23} - r_{32} \\ r_{31} - r_{13} \\ r_{12} - r_{21} \end{pmatrix}$$

which on using (17) gives

$$\dot{\phi} = \omega^t c$$

To get (18b) note that $Rc = c$ and $\|c\| = 1$. Hence

$$\dot{R}c + R\dot{c} = \dot{c}$$

or

$$S(\omega)c = (I - R)\dot{c}$$

which on using (15) becomes

$$S(\omega)c = -\sin \phi S(c)\dot{c} - (1 - \cos \phi)S^2(c)\dot{c}$$

But from (6) $S^2(c) = -I + cc^t$, whereas $c^t\dot{c} = 0$. Hence,

$$S(\omega)c = -\sin \phi S(c)\dot{c} + (1 - \cos \phi)\dot{c} \tag{B1}$$

and

$$S(c)\dot{c} = \frac{(1 - \cos \phi)\dot{c} - S(\omega)c}{\sin \phi}$$

Now premultiply both sides of (B1) by $S(c)$ and simplify to get

$$S(c)S(\omega)c = 2 \tan\left(\frac{1}{2}\phi\right)\dot{c} - \tan\left(\frac{1}{2}\phi\right)S(\omega)c$$

Hence,

$$\dot{c} = \frac{1}{2}S(\omega)c + \frac{1}{2}\cot\left(\frac{1}{2}\phi\right)S(c)S(\omega)c$$

The last term in the above equation is a vector triple product. The matrix form of the vector triple product identity is, for any x, y , and z in E^3 , $S(x)S(y)z = (x^t z)y - (x^t y)z$. Therefore

$$\dot{c} = \frac{1}{2}S(\omega)c + \frac{1}{2}\cot\left(\frac{1}{2}\phi\right)[\omega - (\omega^t c)c]$$

REFERENCES

1. Showman, Robert D.: Simplified Processing of Star Tracker Commands for Satellite Attitude Control. IEEE Transactions on Automatic Control. vol. AC-12, no. 4, Aug. 1967, pp. 353-359.
2. Hansen, Q. Marion; Gabris, Edward A.; Pearson, M. Dale; and Leonard, Barry S.: A Gyroless Solar Pointing Attitude Control System for the Aerobee Sounding Rocket. J. of Spacecraft and Rockets, vol. 4, no. 11, Nov. 1967, pp. 1443-1447.
3. Mortensen, R. E.: On Systems for Automatic Control of the Rotation of a Rigid Body. Rep. 63-23, Electronics Res. Lab., Univ. of Calif., Berkeley, Nov. 27, 1963.
4. Meyer, George: On the Use of Orthogonal Transformation for the Synthesis of Attitude Control Systems. Presented at the 1966 Joint Automatic Control Conference, Seattle, Washington. Preprints of Conference Papers, pp. 430-434.
5. Meyer, George: On the Use of Euler's Theorem on Rotations for the Synthesis of Attitude Control Systems. NASA TN D-3643, 1966.
6. Meyer, George: Response Envelope - A Global Description of Three-Axis Large-Angle Spacecraft Attitude Control Systems. NASA TN D-4896, 1968.
7. Meyer, George: The Design of a Large-Angle Three-Axis Attitude Servo-Mechanism for Spacecraft. Proceedings of the XVIII International Astronautical Congress - Belgrade 1967, vol. 1, pp. 499-505.
8. Dishman, Bruce H.; and Moran, Francis J.: Air Bearing Table Mechanization and Verification of a Spacecraft Wide Angle Attitude Control System. Presented at the AIAA Guidance, Control, and Flight Mechanics Conference, Paper 69-856, 1969.
9. Pontryagin, L. S.; Boltyanskii, V. G.; Gamkrelidze, R. V.; and Mishchenko, E. F.: The Mathematical Theory of Optimal Processes. Interscience Publishers, 1962.

FIRST CLASS MAIL



POSTAGE AND FEES PAID
NATIONAL AERONAUTICS AND
SPACE ADMINISTRATION

POSTMASTER: If Undeliverable (Section 158
Postal Manual) Do Not Return

"The aeronautical and space activities of the United States shall be conducted so as to contribute . . . to the expansion of human knowledge of phenomena in the atmosphere and space. The Administration shall provide for the widest practicable and appropriate dissemination of information concerning its activities and the results thereof."

— NATIONAL AERONAUTICS AND SPACE ACT OF 1958

NASA SCIENTIFIC AND TECHNICAL PUBLICATIONS

TECHNICAL REPORTS: Scientific and technical information considered important, complete, and a lasting contribution to existing knowledge.

TECHNICAL NOTES: Information less broad in scope but nevertheless of importance as a contribution to existing knowledge.

TECHNICAL MEMORANDUMS: Information receiving limited distribution because of preliminary data, security classification, or other reasons.

CONTRACTOR REPORTS: Scientific and technical information generated under a NASA contract or grant and considered an important contribution to existing knowledge.

TECHNICAL TRANSLATIONS: Information published in a foreign language considered to merit NASA distribution in English.

SPECIAL PUBLICATIONS: Information derived from or of value to NASA activities. Publications include conference proceedings, monographs, data compilations, handbooks, sourcebooks, and special bibliographies.

TECHNOLOGY UTILIZATION PUBLICATIONS: Information on technology used by NASA that may be of particular interest in commercial and other non-aerospace applications. Publications include Tech Briefs, Technology Utilization Reports and Technology Surveys.

Details on the availability of these publications may be obtained from:

**SCIENTIFIC AND TECHNICAL INFORMATION OFFICE
NATIONAL AERONAUTICS AND SPACE ADMINISTRATION
Washington, D.C. 20546**